IEEE Access
Multidisciplinary | Rapid Review | Open Access Journal

Received 24 October 2023, accepted 10 November 2023, date of publication 14 November 2023,
date of current version 22 November 2023.

Digital Object Identifier 10.1109/ACCESS.2023.3333254

RESEARCH ARTICLE

Enhancing Multi-Band MIMO Antenna Stability for Various Electronic Applications With Human-Body Interaction Consideration

MING-AN CHUNG, (Member, IEEE), CHIA-CHUN HSU, MING-CHANG LEE, AND CHIA-WEI LIN

Department of Electronic Engineering, National Taipei University of Technology, Taipei 106, Taiwan

Corresponding author: Ming-An Chung (mingannchung@mail.ntut.edu.tw)

This work was supported by the National Science and Technology Council, Taiwan, under Grant NSTC 112-2221-E-027-065-.

ABSTRACT This paper proposes a multi-band antenna suitable for LTE and 5G NR frequency bands. The multi-band antenna is designed on a 60-mm × 12.5-mm FR4 substrate without requiring passive components. The multi-band antenna uses a coupled-feed structure to reach the LTE900 frequency band, while the rest of the working frequency bands are implemented using a monopole antenna. multi-band antennas are implemented on electronic devices like smartphones, tablets, and laptops to form Multiple-Input Multiple-Output (MIMO) systems. Each multi-band antenna maintains consistency in measurement and simulation, with isolation below −10 dB, showcasing its robustness. The MIMO antenna system's envelope cross-correlation remains below 0.5 across various devices, indicating stable performance. The above characteristics validate the multi-band antenna's applicability to diverse-sized portable electronics. Furthermore, Specific Absorption Rate (SAR), assessing radiation's impact on humans, is considered. Simulations of SAR for different MIMO antenna systems near the head, hand, or leg consistently meet safety standards, ensuring that MIMO antenna systems pose no radiation threat to human health.

INDEX TERMS LTE, 5G, multi-band, MIMO antenna, coupled-feed.

I. INTRODUCTION

With the continuous advancement of modern communication technology, fifth-generation (5G) communication technology has been born under the social demand for the internet and electronic communication equipment to meet the growing demand for communication transmission. In addition, the Multiple-Input Multiple-Output (MIMO) antenna system has the characteristics of increasing channel capacity and spectrum efficiency. As channel capacity increases, so does the transmission rate of the MIMO antenna system, allowing it to satisfy high-throughput and high-rate transmission requirements [1], [2], [3], [4], [5]. Therefore, MIMO antenna technology based on multi-antenna transmission has attracted a lot of attention [6], [7], [8], [9], [10].

The reason is that MIMO antenna technology is to set multiple antennas in communicating electronic devices such as smartphones, tablets, and laptops. As the size of communication electronic equipment gradually decreases, it becomes difficult to design antennas in the limited area of communication electronic equipment. In the same time, it is difficult to maintain good isolation between antennas in a small space because the antennas can interfere with each other and affect signal transmission [11], [12], [13], [14], [15], [16].

This paper discusses some antenna design research in recent years and lists the following issues:

1) In recent years, due to the popularity of 5G communication technology, there are many antenna designs used in Sub-6G and 5G NR frequency bands that are worthy of reference. In [17], the H-shaped monopole antenna for laptop was proposed. This antenna can be installed on the laptop without an additional ground plane and uses an ultra-thin size to reach the 5G NR band, which is a very suitable application for modern ultra-thin laptops. In [18], a 4 × 4 MIMO antenna system for smartphones was designed. The antenna is composed of four

The associate editor coordinating the review of this manuscript and approving it for publication was Giorgio Montisci.

© 2023 The Authors. This work is licensed under a Creative Commons Attribution-NonCommercial-NoDerivatives 4.0 License.
For more information, see https://creativecommons.org/licenses/by-nc-nd/4.0/

octagonal ring structures and is designed on a flexible substrate. This antenna can show good antenna performance in both WLAN and Sub-6G. At the same time, the impact of SAR on the human body has also been analyzed in the literature, showing the flexibility of this antenna in smartphones. Therefore, it can be understood that antennas for current portable communication devices tend to be designed in high-frequency bands, such as the Sub-6G or 5G NR frequency bands [2], [6], [10], [19], [20], [21]. However, such a trend neglects LTE and other low-frequency bands, making the application range of antennas on communication devices relatively simple.

2) To make the designed antenna have more transmission frequency bands, some literature combines more than two frequency bands into a single antenna (such as LTE and Sub-6G) to achieve multi-band data transmission [14], [15], [22], [23], [24], [25]. However, the low-frequency bands (below 1 GHz) require longer wavelengths, which can make the antenna structure overly complex within limited space or necessitate passive components to achieve the LTE frequency band. This method increases the cost and complexity of antenna design and manufacture.
3) Currently, the design space for antennas within communication devices is continuously shrinking, posing a challenge to achieve high isolation between antennas in MIMO antenna systems. As a solution to enhance isolation, certain studies have proposed the simultaneous use of two different antenna structures to realize a multi-band MIMO antenna system [26], [27]. This approach takes advantage of the characteristic of a smaller overall area for high-frequency antennas and the requirement for a larger area for low-frequency antennas. A MIMO antenna system is formed when antennas of different frequency bands are placed at different positions within the communication device. However, achieving effective isolation becomes difficult due to the limited space in communication devices and the close proximity of antennas.

According to the problems discussed above, it is considered that MIMO antennas currently used in mobile communication equipment should have the following characteristics:

1) Different frequency bands are concentrated in one antenna to increase the overall practicability of the antenna, so the antenna itself has multiple frequency bands. Then use this antenna to configure the MIMO antenna system for electronic devices of different sizes, to achieve multi-band and multi-channel transmission performance.
2) The multi-band antenna should be designed in a planar structure, and use the coupled-feed structure to realize the LTE frequency band without using passive components as much as possible [9], [28]. This design method can make the antenna realize the low-frequency band with a more straightforward structure, and the low-frequency band is not easily affected by the high-frequency branch to cause frequency deviation. In addition, the position of the frequency band on the antenna branch can be judged more clearly, and the antenna frequency band can be adjusted more quickly.
3) A MIMO antenna system that meets the above two conditions can directly optimize isolation by changing the antenna position and keeping all antennas' isolation below −10dB [29]. In other literature, −10dB or less is also used as the antenna isolation standard of the antenna [2], [4], [5], [7], [8], [12], [13], [26], [28], [29].

This paper proposes a multi-band antenna that realizes the LTE900 frequency band through the coupled-feed structure without using passive components. At the same time, the antenna can also cover high-frequency bands such as Sub-6G and WiFi 7. The simulation and measurement analysis of the multi-band antenna has very similar results, which proves that the stable structural characteristics of the multi-band antenna can quickly design MIMO systems on various electronic devices such as smartphones, tablets, and laptops. Therefore, the isolation of the MIMO antenna system can be optimized by changing the position of each multi-band antenna. In this paper, MIMO antenna systems on different electronic devices use FR-4 substrates for planar design. The manufacturing process is easy and low-cost and will not cause radiation damage to the human body. This paper will introduce the results of the multi-band antenna structure design and evolution simulation in Section II. Section III analyzes and compares the performance of MIMO antenna systems through simulation and measurement. Section IV discusses the radiation effects of MIMO antenna systems on the human body on different devices, and the research results of MIMO antenna systems are compared with similar references. Finally, Section V summarizes the results and conclusions for MIMO antenna systems.

II. PROPOSED MULTI-BAND ANTENNA SYSTEM DESIGN

A. PROPOSED ANTENNA DESIGN DIMENSIONS AND BRANCH ANALYSIS

Fig. 1 depicts the design structure of the multi-band antenna suggested in this research, and Table 1 depicts the antenna's precise dimensions. The multi-band antenna proposed in this paper adopts a monopole antenna structure and is designed on an FR4 substrate with a plane size of 12.5 mm × 60 mm × 0.8 mm (dielectric constant is 4.4 and loss tangent is 0.02). The design of the multi-band antenna branch is shown in Fig. 2.

The low-frequency band needs to correspond to a longer wavelength. Therefore, in order not to complicate the multi-band antenna structure, the low-frequency part adopts a coupled-feed structure to radiate current to the ground line, coupling the 860-940 MHz frequency band in this way, as shown in Fig. 2 from point A to point B. To make the low-frequency cover more LTE frequency bands, the frequency band of 950-1060 MHz is coupled out by adjusting the width of the branch, as shown from point A to point C

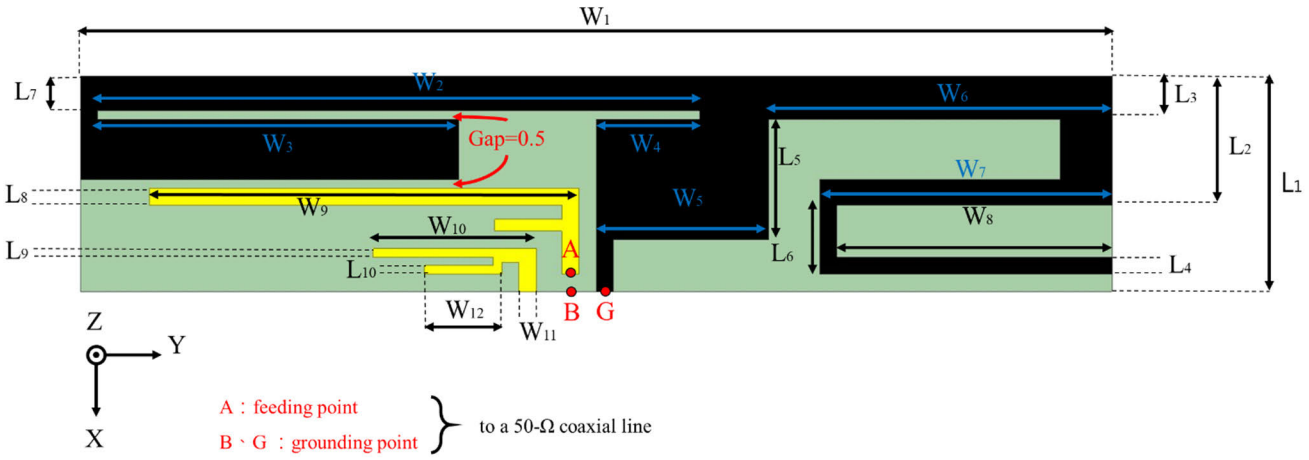

FIGURE 1. Proposed multi-band antenna size structure.

TABLE 1. Proposed multi-band antenna detailed dimensions table.

Parameter	Value(mm)	Parameter	Value(mm)
W_1	60	W_{12}	1
W_2	35	L_1	12.5
W_3	21	L_2	7.5
W_4	6	L_3	3
W_5	10	L_4	1
W_6	20	L_5	7
W_7	17	L_6	4
W_8	16	L_7	2
W_9	25	L_8	1
W_{10}	9.5	L_9	0.5
W_{11}	4.5	L_{10}	0.5

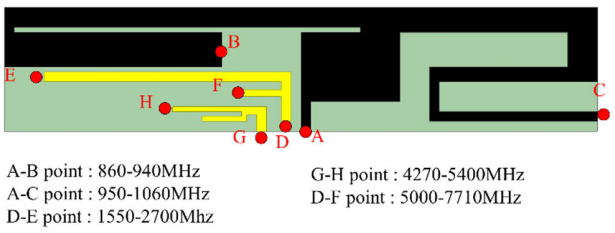

FIGURE 2. Analysis of the proposed multi-band antenna branch.

in Fig. 2. The Sub-6G frequency band is coupled to the 4270-5000 MHz frequency band by the L-shaped antenna next to the feed point, as shown from point G to point H in the figure. In addition, the short branch from point D to point F couples out the 5000-7710 MHz frequency band covering WiFi 7. Finally, connect the multi-band antenna to the metal ground plane with a 50-ohm coaxial cable, as shown at point G in the Fig.2. This is the branch analysis process of the multi-band antenna.

B. ANTENNA EVOLUTION

This section uses antenna simulation software to simulate and analyze the evolution steps of the designed multi-band antenna, as shown in Fig. 3. Fig. 3(a) shows the evolution

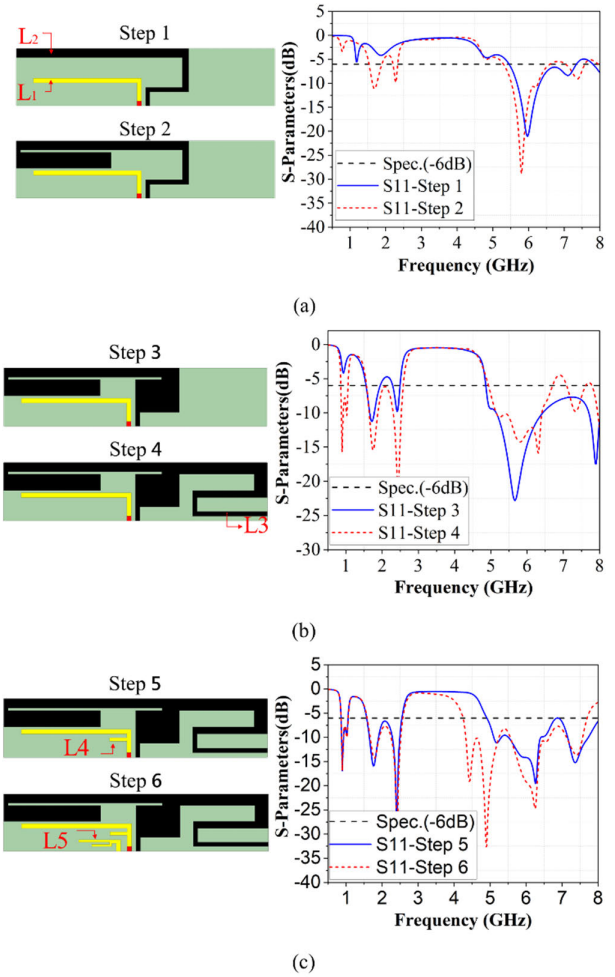

FIGURE 3. Evolution steps of the proposed multi-band antenna structure: (a)steps 1 to 2, (b)steps 3 to 4 and (c)steps 5 to 6.

process of the multi-band antenna from step 1 to step 2. In step 1 a 60 mm × 12.5 mm × 0.8mm rectangle was

designed as the FR-4 substrate to connect to the metal ground plane of the laptop. The feed point is designed under the FR4 substrate and in contact with the metal ground plane of the laptop, and an L-shaped branch L_1 extends from the feed point. In addition, a curved branch L_2 with a total length of 57 mm is extended from 0.5 mm to the right side of the feed point for simulation. The S_{11} of the multi-band antenna in step 1 shows that the resonance frequency bands with reflection coefficients below −6 dB are 1.1 and 1.9 GHz. At the same time, the multi-band antenna generates a frequency band covering the range of 5.45 to 7.34 GHz. In step 2, the resonance frequency band of the multi-band antenna is shifted to 1.7-2.4 GHz (bandwidth is about 360 MHz) when the reflection coefficient S_{11} is lower than −6dB, the high frequency 5.98 GHz generated in step 1, and is retained in the −7.11 GHz frequency band.

Fig. 3(b) illustrates the evolutionary process from Step 3 to Step 4. In Step 3, the width of the L_2 front-end is increased, resulting in the multi-band antenna generating a resonant frequency at 980 MHz, with the S_{11} reflection coefficient meeting the standard of being below −6 dB. Meanwhile, the frequency bands generated by the multi-band antenna's S_{11} in Steps 1-2, namely 1.7, 2.4, 5.98, and 7.11 GHz, are still present. Step 4 involves the generation of a resonant frequency range from 900 MHz −1.03 GHz (approximately 200 MHz bandwidth) through the use of the differently sized curved branch, L_3, on the right side. Additionally, in Step 4, the frequency range of 1.71 and 2.4 GHz is expanded to 1.57-2.58 GHz.

Fig. 3(c) shows the evolution process from step 5 to step 6.

Step 5 adds a 3.9mm short branch L_4 to the L_1 branch to increase the bandwidth above 5G while retaining the frequency bands of 860-1060 MHz and 1.58-2.58 GHz. In step 6, in order to realize the working frequency band of Sub-6G, add an L-shaped branch L_5 at 1.5mm to the left of the feeding point. Extend the multi-band antenna high frequency band from 4.25-7.7 GHz. After the above adjustments, the proposed multi-band antenna effectively covers multiple operating frequency bands, including LTE, 2.4 GHz, Sub-6 G, and WiFi 7.

C. PROPOSED CONFIGURATION OF MIMO ANTENNA SYSTEM ARCHITECTURE

The MIMO antenna system proposed in this paper can be applied to electronic devices such as smartphones, tablets, and laptops, and its configuration framework is shown in Figs. 4-5. The MIMO antenna system is designed on a 15-inch laptop with a size of 330mm x 220mm and consists of 10 identical multi-band antennas arranged with a distance of 20mm between antennas, as shown in Fig. 4. Additionally, the dimensions of smartphones and tablets are 2 × 2 MIMO antenna systems of 70 mm×120 mm and 10 × 10 MIMO antenna systems of 260 mm×200 mm, as shown in Fig. 5.

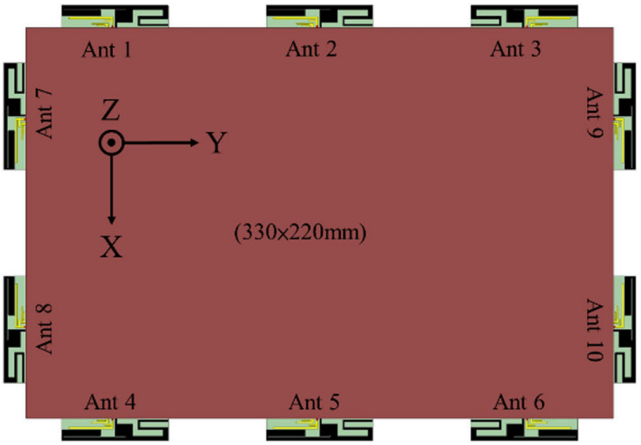

FIGURE 4. The proposed setup of the MIMO antenna system.

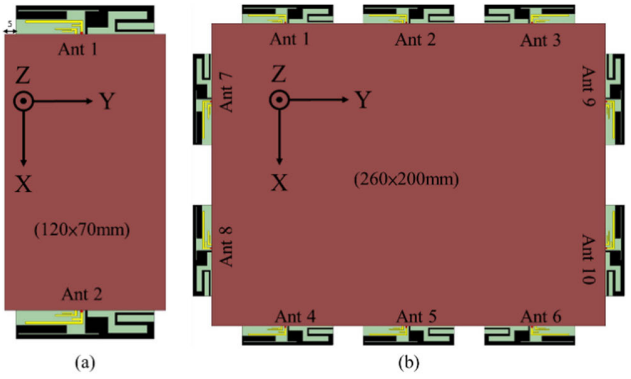

FIGURE 5. Configurations of the MIMO antenna system on different devices: (a)smartphone and (b)tablet.

D. SURFACE CURRENT ANALYSIS OF THE MIMO ANTENNA SYSTEM

The operational principle of an antenna relies on the current flowing into the antenna from the feed point. The current is distributed among different branches of the antenna, each tailored to achieve impedance matching for specific frequency bands, resulting in the generation of radiating electromagnetic waves.

Figs. 6-8 show simulated surface current distributions for MIMO antenna systems. When the frequency is 900 MHz of Ant.1 in the MIMO antenna system, the current converges in the L2 branch as shown in Fig. 6(a). In Fig. 6(b), when the frequency is 1 GHz, the current flows to the right L3 branch to generate a resonance frequency band of 1.03 GHz. In the antenna system, the frequency is 1.76 GHz of Ant.1 exhibits concentrated current on the L1 branch, as shown in Fig. 6(c), while at a frequency of 2.4 GHz, the current flows concentratedly between the two ends of L1 and L2, as shown in Fig. 6(d). When Ant.1 is at 4.43 GHz frequency, the current converges on the L-shaped branch on the left side of the feeding point to generate a 4.2-4.9 GHz, as shown in Fig. 6(e). At 4.8 GHz, the currents converge at L_1 close to the feed point to generate a frequency band of 6.25-7.4 GHz. The above

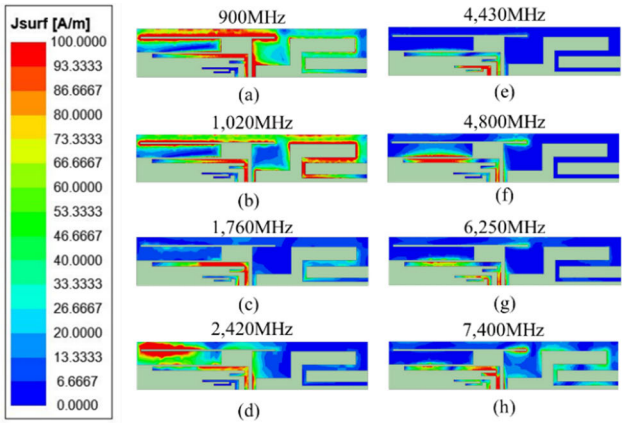

FIGURE 6. Simulated surface current distribution at different frequencies for the proposed MIMO antenna system Ant.1: (a)900 MHz, (b)1020 MHz, (c)1760 MHz, (d)2420 MHz, (e)4430 MHz, (f)4800MHz, (g)6250 MHz and (h)7400 MHz.

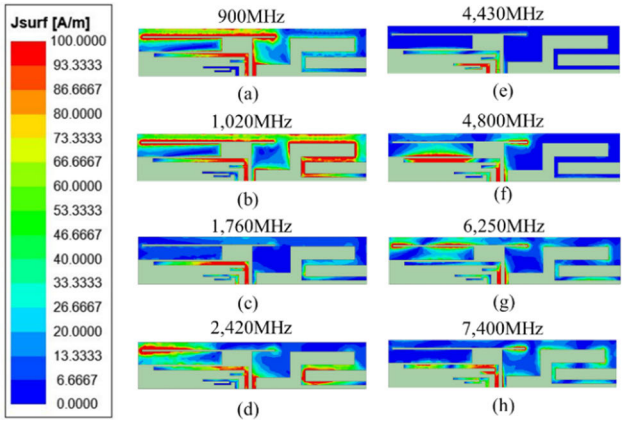

FIGURE 7. Simulated surface current distribution at different frequencies for the proposed MIMO antenna system Ant.2: (a)900 MHz, (b)1020 MHz, (c)1760 MHz, (d)2420 MHz, (e)4430 MHz, (f)4800MHz, (g)6250 MHz and (h)7400 MHz.

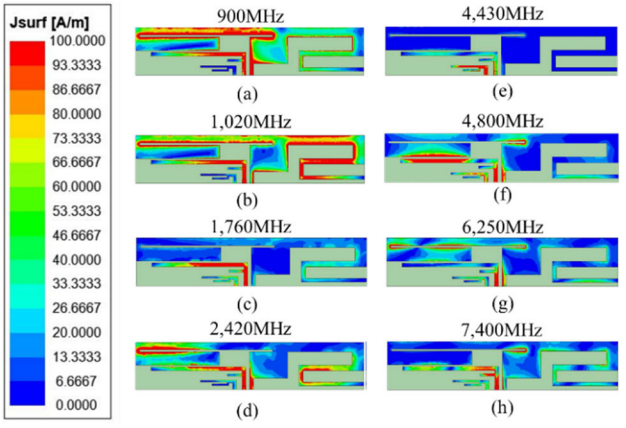

FIGURE 8. Simulated surface current distribution at different frequencies for the proposed MIMO antenna system Ant.7: (a)900 MHz, (b)1020 MHz, (c)1760 MHz, (d)2420 MHz, (e)4430 MHz, (f)4800MHz, (g)6250 MHz and (h)7400 MHz.

multi-band surface current analysis is consistent with the results shown by the evolution of multi-band antennas.

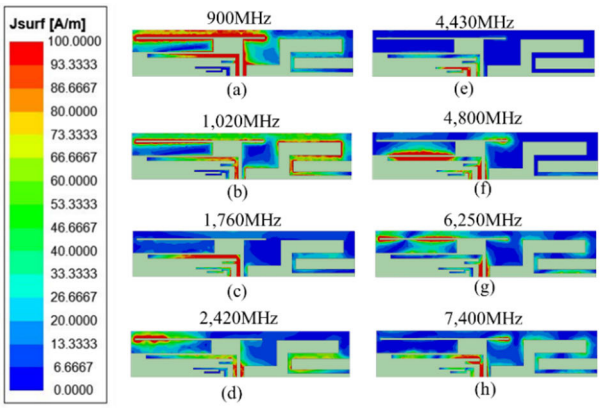

FIGURE 9. Simulated surface current distribution at different frequencies for the proposed smartphone MIMO antenna system Ant.1: (a)900 MHz, (b)1020 MHz, (c)1760 MHz, (d)2420 MHz, (e)4430 MHz, (f)4800MHz, (g)6250 MHz and (h)7400 MHz.

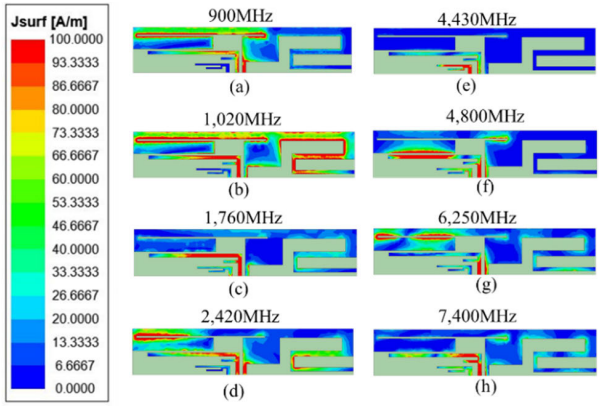

FIGURE 10. Simulated surface current distribution at different frequencies for the proposed tablet MIMO antenna system Ant.1: (a)900 MHz, (b)1020 MHz, (c)1760 MHz, (d)2420 MHz, (e)4430 MHz, (f)4800MHz, (g)6250 MHz and (h)7400 MHz.

In Figs. 7-8, the simulated surface current distribution of Ant.2 and Ant.7 within the MIMO antenna system closely resembles that of Ant.1 because this similarity is due to the fact that Ant.1, Ant.2, and Ant.7 all utilize the same structure of the multi-band antenna. The antennas within the MIMO antenna system exhibit symmetry or mirror relationships. Specifically, Ant.1 and Ant.3, Ant.7 and Ant.8 are in symmetric relationships, while Ant.1 and Ant.4, Ant.2 and Ant.5, Ant.7 and Ant.8, Ant.9 and Ant.10 are mirror relationships. Therefore, the simulation results for Ant.1, Ant.2, and Ant.7 represent the simulation results for all Multi- Band antennas in the system.

Figs.9 and 10 show the results of simulating the surface current of the MIMO antenna system on electronic devices of different sizes. Even if the system is applied to smartphones and tablets, the surface current distribution presented by it is also similar to that of the surface current distribution of a laptop is very similar. Due to the relatively smaller grounding area of smartphones, the surface current intensity at 900MHz frequency is slightly weaker in simulation. However, the overall current flow direction is the same as that of laptop and tablet computers. The above analysis results show that the

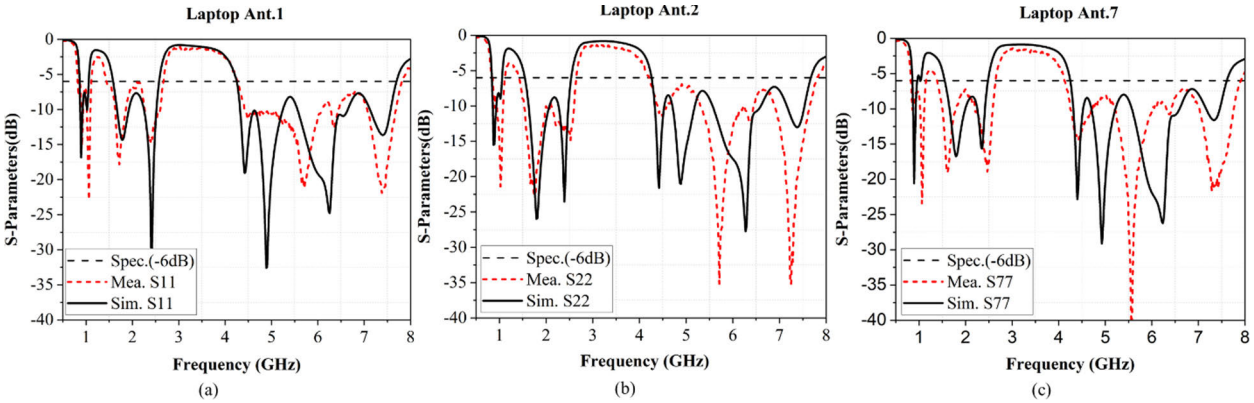

FIGURE 11. Results of simulation and measurement of the reflection coefficient of the proposed MIMO antenna system: (a)S_{11}, (b)S_{22} and (c)S_{77}.

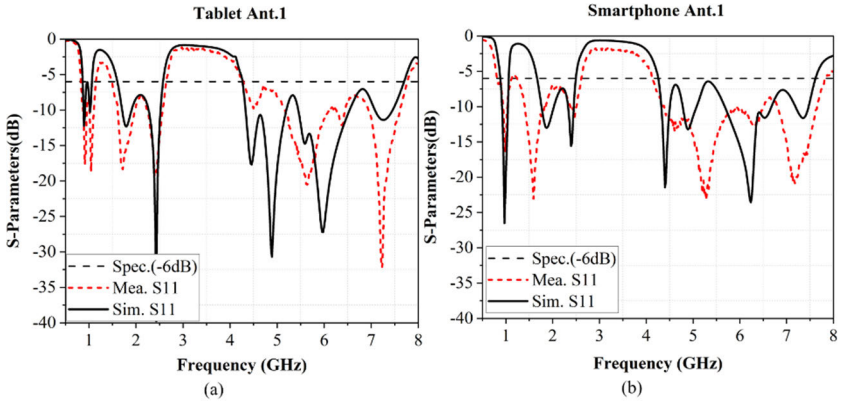

FIGURE 12. Results of simulation and measurement of the proposed MIMO antenna system on different electronic devices: (a)tablet and (b)smartphone.

antenna structure in multi-band MIMO antenna can stabilize the current flow, making the MIMO antenna system less susceptible to equipment size changes affecting the operating frequency band. Furthermore, this also confirms the practicality of the application of the MIMO antenna system in various electronic devices.

III. ANTENNA ANALYSIS

A. ANTENNA S-PARAMETER ANALYSIS

Each multi-band antenna has a symmetrical or mirror relationship with each other in the MIMO antenna system, so these multi-band antennas show highly similar measurement and simulation results. In the MIMO antenna system configuration, whether it is a laptop, a tablet, or a smartphone, it is composed of the same multi-band antenna. The only difference between these devices is that the size of the ground plane is different. Therefore, only Ant.1, Ant.2, and Ant.7 are needed to express the simulation and measurement results of the reflection coefficients of all antennas.

Fig. 11(a) is the S_{11} simulation and measurement results of the laptop Ant.1. In the simulation process, the frequency bands of Ant.1 are 820-1100 MHz (bandwidth is about 290 MHz), 1.44-2.67 GHz (bandwidth is about 1230 MHz), and 4.27-7.82 GHz (bandwidth is about 3010 MHz), and produces resonance points below −6 dB at 900 MHz and 1.02, 1.76, 2.42, 4.43, 6.25, 7.4 GHz. In the process of measurement, the frequency bands of Ant.1 are 820-1100 MHz (the bandwidth is about 290 MHz), 1.44-2.67 GHz (the bandwidth is about 1230 MHz), and 4.27-7.82 GHz (the bandwidth is about 3010 MHz), and produces resonance points below −6 dB at 920 MHz and 1.06, 1.73, 2.4, 4.51, 5.72, 7.4 GHz. The reflection coefficients of Ant.2 and Ant.7 are shown in Fig. 11(a) and 11(b), respectively. It can be seen from Fig. 11(a) and 11(b) that the reflection coefficient simulation and measurement results of Ant.2 and Ant.7 are very similar to those of Ant.1. It is verified that no matter how the antenna position of the MIMO antenna system is adjusted, the frequency band change will not be affected. Additionally, when different numbers of multi-band antennas are deployed on smartphones and tablets with different ground plane sizes, the measured and simulated reflection coefficients show the same frequency band trend, as shown in Figs. 12(a) and 12(b). The above results show that the number of antennas configured or the size of the ground plane does not affect the frequency band of the MIMO antenna system.

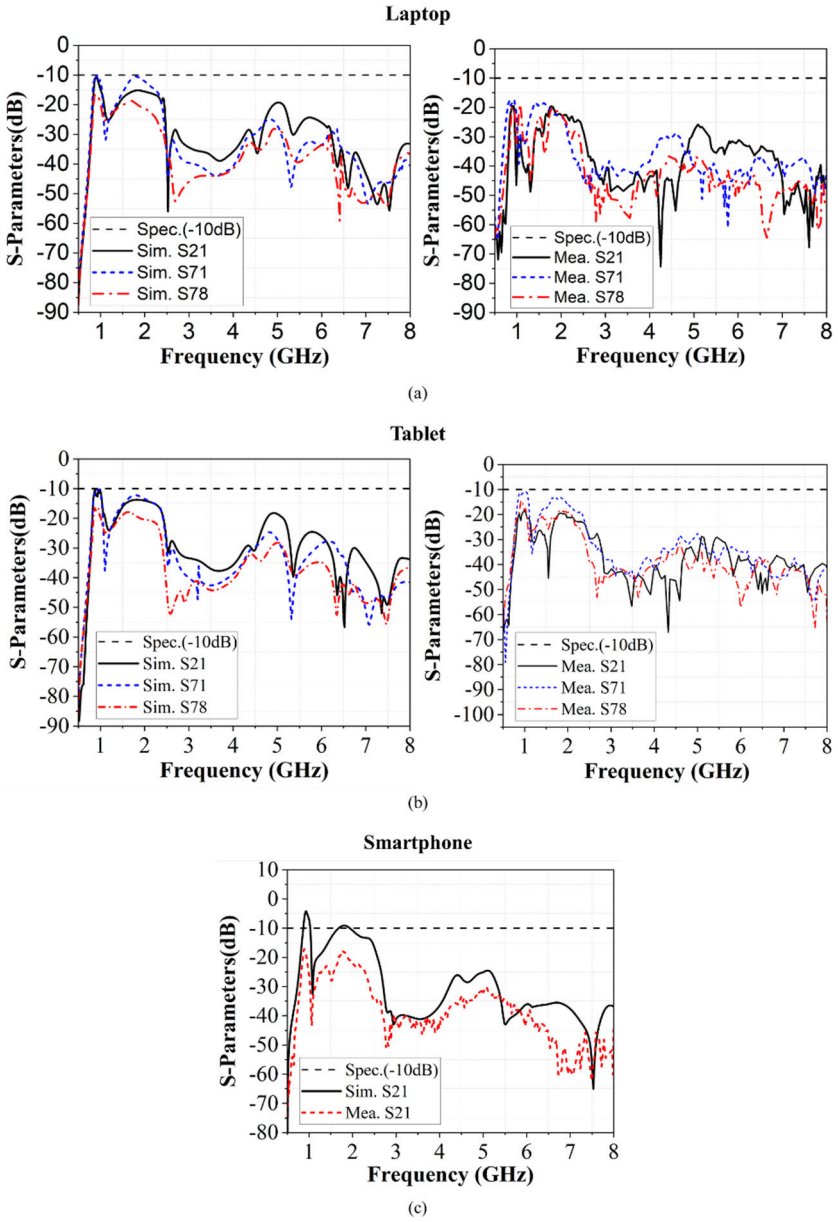

FIGURE 13. MIMO antenna system isolation simulation and measurement results: (a)laptop, (b)tablet and (c)smartphone.

Fig. 13 illustrates the simulated and measured isolation results of the MIMO antenna system on different electronic devices. In Fig. 13, the isolation levels of the MIMO antenna system on the laptop are all below −10 dB, indicating favorable antenna-to-antenna isolation performance. Within the MIMO antenna system, it is observed that each multi-band antenna needs to be separated by at least 20 mm to achieve optimal isolation. Given the mirror relationships between Ant.1-Ant.3 and Ant.4-Ant.6, as well as Ant.7-Ant.8 and Ant.9-Ant.10, the isolation results of Ant.1-Ant.2, Ant.1-Ant.7, and Ant.7-Ant.8 in Figs. 13(a) and 13(b) can represent the isolation performance of all antenna combinations within the MIMO antenna system.

The antenna isolation represents as (1) and (2) [30].

$$I_H\,|dB| = 22 + 20lg\frac{dh}{\lambda} - [G_{Tx}(\varphi) + G_{Rx}(\varphi)] \quad (1)$$

$$I_v\,[dB] = 28 + 40\lg(1/\lambda) \quad (2)$$

As depicted in Figs. 13(a) and (b), both the laptop and tablet exhibit very similar isolation levels at low frequency, approximately −10 dB. On the other hand, the simulated results for the MIMO antenna system in smartphones at low frequencies only reach -5 dB. This discrepancy may be attributed to the smaller ground plane area in the smartphones, which reduces the antenna spacing and consequently results in a simulated isolation level very close to −5 dB. So, the result of

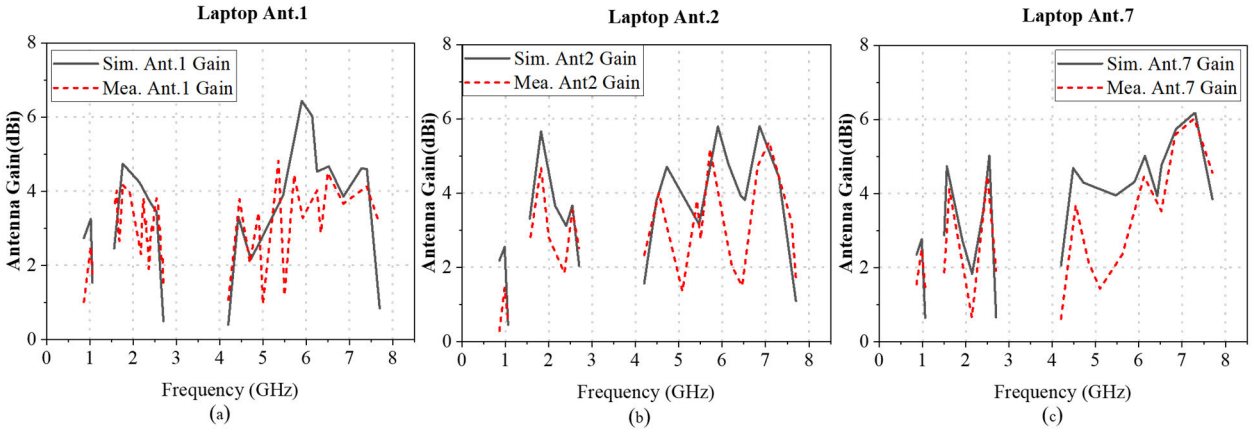

FIGURE 14. Gain results of simulation and measurement results of the MIMO antenna system for laptop: (a)Ant.1, (b)Ant.2 and (c)Ant.7.

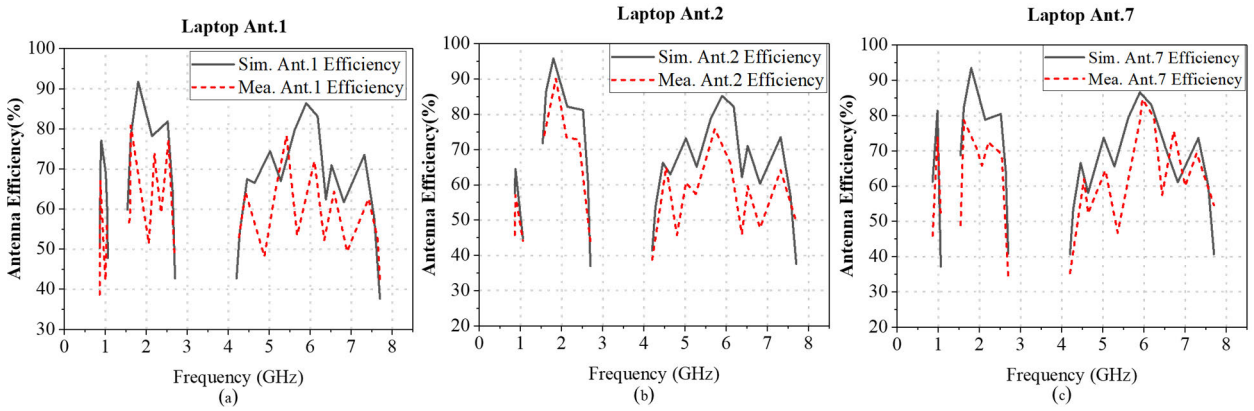

FIGURE 15. Efficiency results of simulation and measurement results of the laptop MIMO antenna system: (a)Ant.1, (b)Ant.2 and (c)Ant.7.

isolation is the same with (1) and (2). However, measurement results for the MIMO antenna system in smartphones can still achieve isolation levels below −10 dB, even approaching −20 dB, as demonstrated in Fig. 13(c). It shows that, despite the smaller ground plane area in smartphones, the overall isolation remains below −10 dB, and in some cases, can even approach −20 dB, as shown in Fig. 13(c).

B. ANALYSIS OF ANTENNA GAIN AND EFFICIENCY

Fig. 14(a) shows the simulated peak gain values in the MIMO antenna system on the laptop for Ant.1 at frequencies of 900 MHz and 1.02, 1.76, 2.42, 4.43, 6.25, and 7.4 GHz are 2.7, 3.2, 4.7, 3.7, 3.3, 4.5, and 4.5 dBi, while the measured peak gain values are 1.0, 2.5, 4.1, 2.7, 3.8, 4.0, and 4.1 dBi.

Fig. 15(a) shows the simulated efficiencies in the MIMO antenna system on the laptop for Ant.1 at frequencies of 900 MHz and 1.02, 1.76, 2.42, 4.43, 6.25, and 7.4 GHz are 77, 68, 92, 81, 67, 83, 73%, respectively, while the measured efficiencies are 62, 48, 80, 59, 64, 71, and 62%.

According to the results, the MIMO antenna system's highest efficiency is close to 62% at low frequencies (below 1 GHz) and about 71% at high frequencies (above 1 GHz). Additionally, Ant.1, Ant.2, and Ant.7 have the same antenna structure, so the gain simulation the same structure, the resonant modes of the antennas will have a very similar tendency. The MIMO and measurement results demonstrate consistent outcomes. In the same time, the gain and efficiency results when the multi-band MIMO antennas are configured on tablets and smartphones also show the same trends as that of laptop MIMO antenna systems, as shown in Figs. 16 and 17.

C. ANALYSIS OF ANTENNA RADIATION PATTERNS

It can be seen from Section III-A that there is a symmetrical or mirror relationship between each multi-band antenna of the MIMO antenna system. Each multi-band antenna has the same antenna structure, so the resonance mode of the antenna has a very similar trend, and the same is true for the radiation pattern of the MIMO antenna system. As shown in Fig. 18, the antenna system was measured based on the XYZ axis set up in the chamber, and the same XYZ axis settings were used for simulation in the electromagnetic simulation software.

Fig. 19 is a 2D gain radiation pattern diagram of the MIMO antenna system on the XY, XZ and YZ planes.

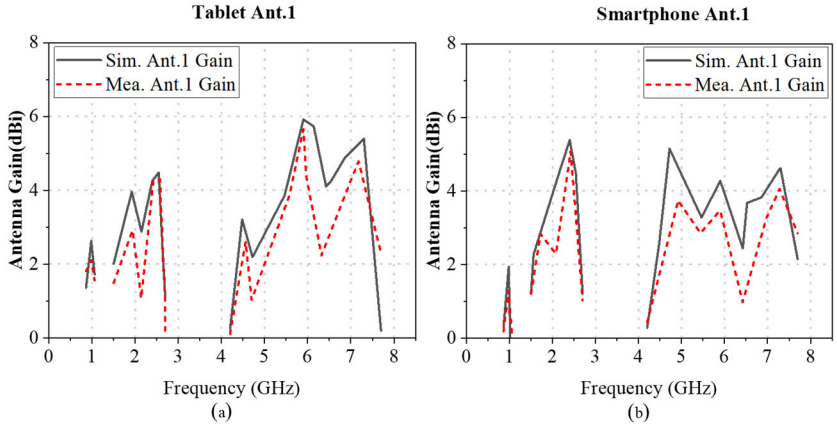

FIGURE 16. Gain results of simulation and measurement results of the MIMO antenna system: (a)tablet Ant.1 and (b)smartphone Ant.1.

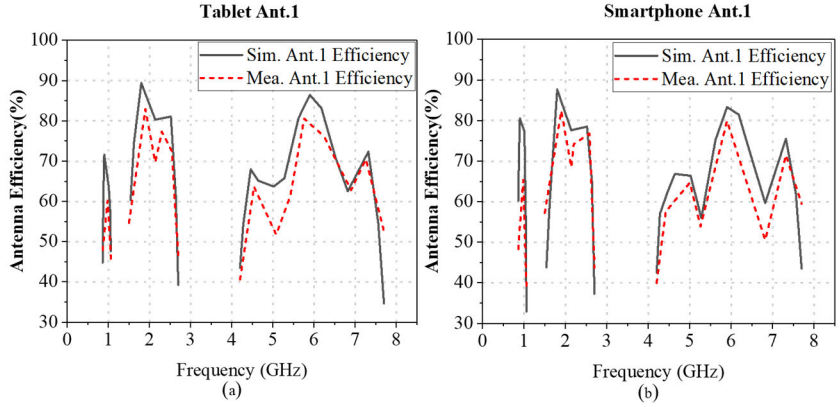

FIGURE 17. Efficiency results of simulation and measurement results of MIMO antenna system: (a)tablet Ant.1 and (b)smartphone Ant.1.

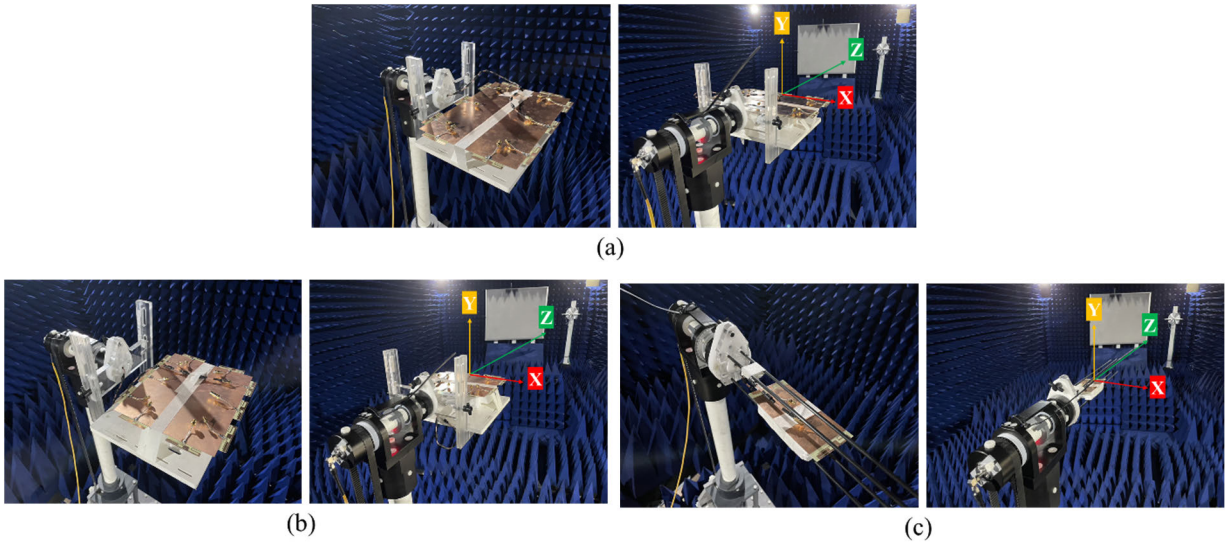

FIGURE 18. MIMO antenna system measurement far-field erection photos: (a)laptop, (b)tablet and (c)smartphone.

It can be seen from the radiation pattern that the simulation and measurement results of the MIMO antenna system at frequencies of 900 MHz and 1.02, 1.76, 2.42, 4.43, 6.25, 7.4 GHz all present similar radiation trends,

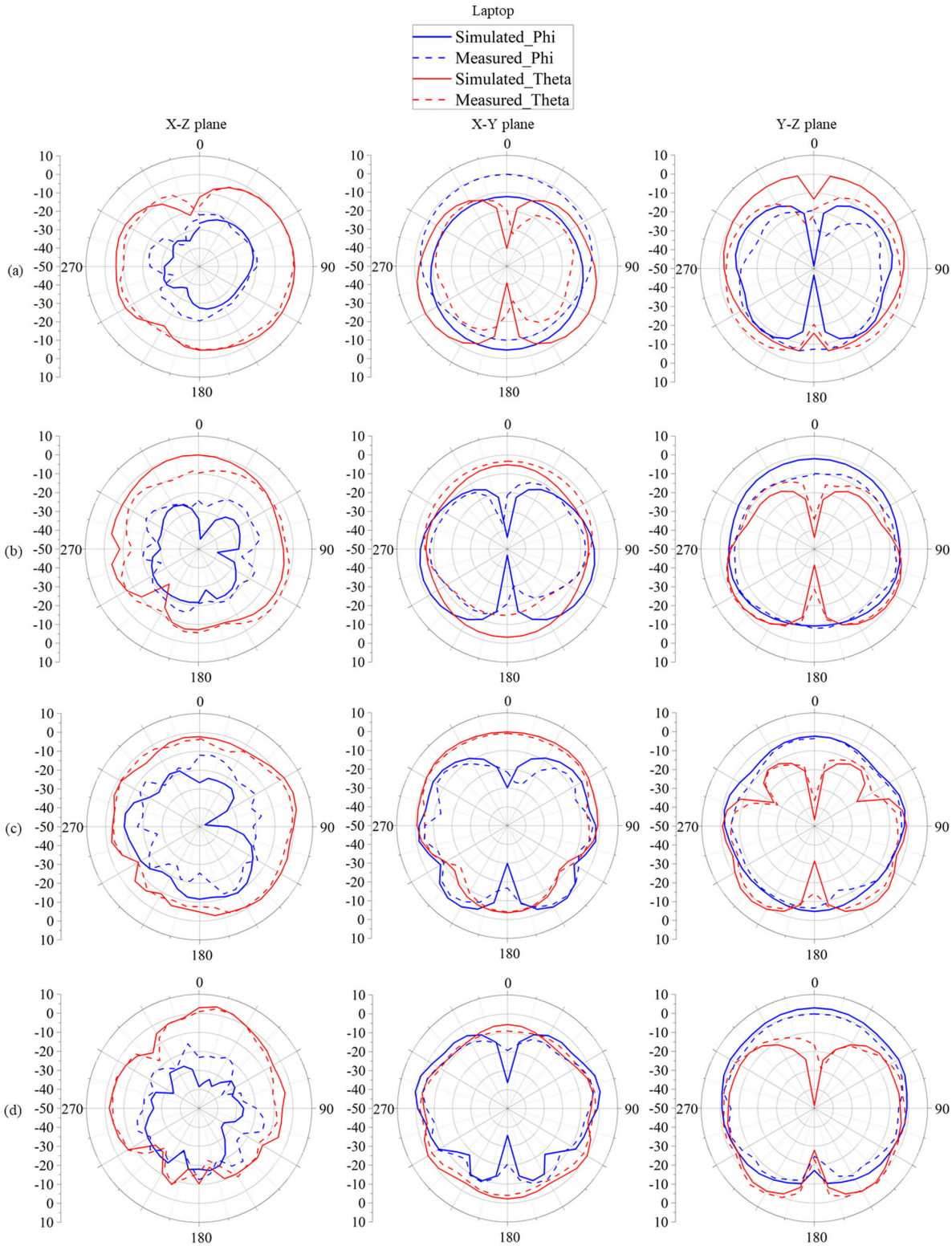

FIGURE 19. 2D Radiation pattern of a laptop MIMO antenna system: (a)900 MHz, (b)1020 MHz, (c)1760 MHz, (d)2420 MHz, (e)4430 MHz, (f)6250 MHz and (g)7400 MHz.

which verifies that the MIMO antenna system can stably transmit multichannel signals. Furthermore, the MIMO antenna system is configured for tablets and smartphones, and the predicted and observed gain radiation patterns demonstrate an excellent omnidirectional trend, as illustrated in Figs. 20 and 21.

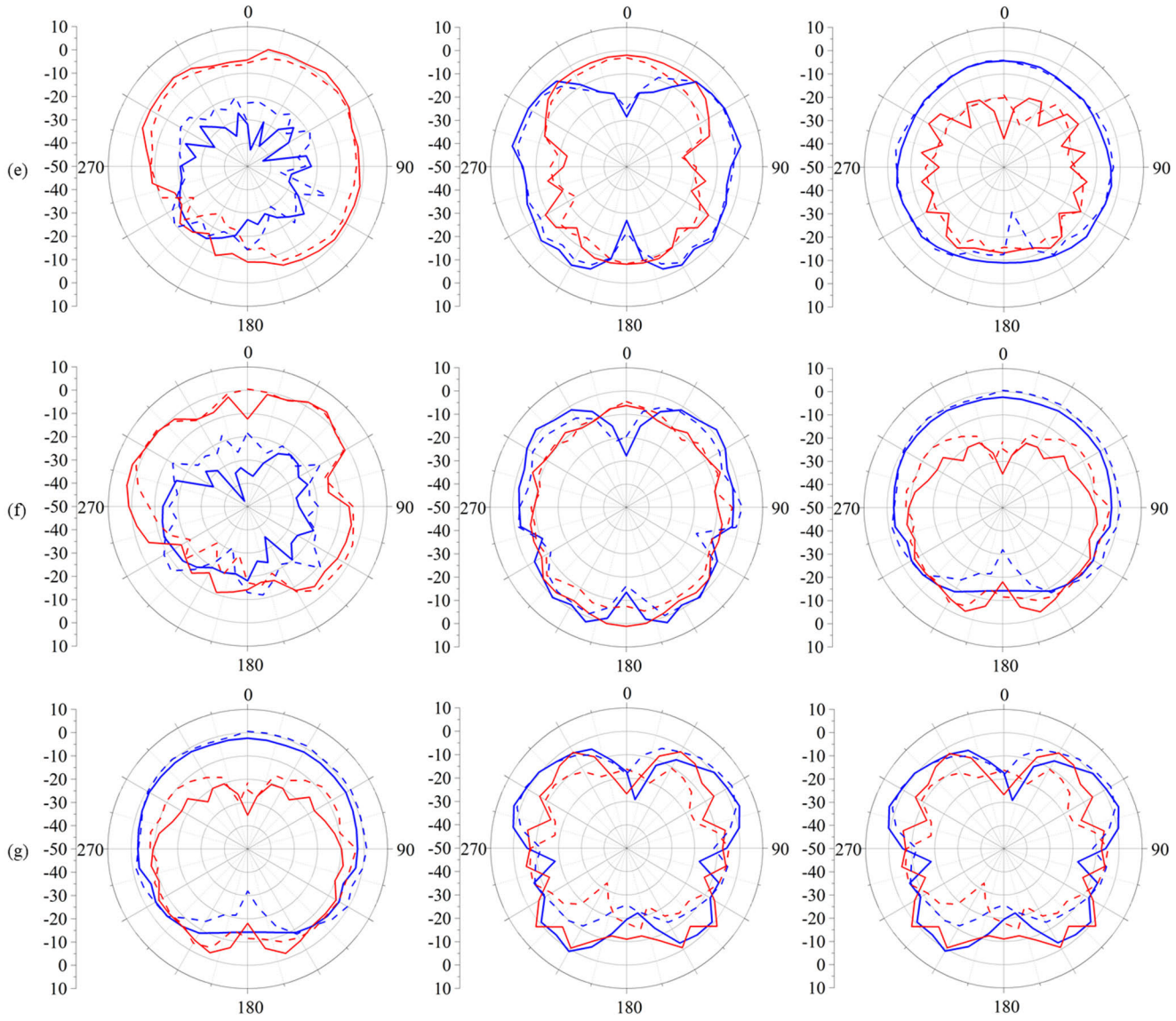

FIGURE 19. *(Continued.)* **2D Radiation pattern of a laptop MIMO antenna system: (a)900 MHz, (b)1020 MHz, (c)1760 MHz, (d)2420 MHz, (e)4430 MHz, (f)6250 MHz and (g)7400 MHz.**

D. ENVELOPE CROSS-CORRELATION (ECC)

ECC is a performance metric that is used to evaluate antennas and is often used to measure the correlation between different antennas in an antenna array, especially in MIMO antenna communication systems or radar systems. The simulated and measured results of ECC for a MIMO antenna system in free space are shown in Figure 22(a). Currently, the overall ECC of the MIMO antenna system is below 0.5, with ECC values slightly higher in the frequency range below 1.5 GHz compared to other frequency bands. This issue can be explored by examining the formula for calculating ECC, as presented in (3) [31]

$$\mathrm{ECC} = \frac{\left|S_{ii}^{*}S_{ij} + S_{ji}^{*}S_{jj}\right|^{2}}{\left(1 - \left(|S_{ii}|^{2} + |S_{ji}|^{2}\right)\right)\left(1 - \left(|S_{jj}|^{2} + |S_{ij}|^{2}\right)\right)} \quad (3)$$

In this paper, a compact, planar, and MIMO design approach was adopted. Implementing any of the aforementioned methods may potentially deviate from the original design requirements. With the criterion for ECC consistently below 0.5 [2], [12], [13], [27], [31], the overall ECC of the MIMO antenna system in this paper is all below 0.5. This indicates that the MIMO antenna system in this paper possesses independent and satisfactory antenna performance. Therefore, no further measures were taken to improve ECC performance.

In addition, due to the mirror and symmetric relationship between each multi-band antenna, the ECC analysis of Ant.1-Ant.2, Ant.1-Ant.7 and Ant.7-Ant.8 can represent all MIMO antenna systems' ECC results. Furthermore, as observed in Figs. 22 (a) and 22(b), the MIMO antenna system demonstrates remarkably similar

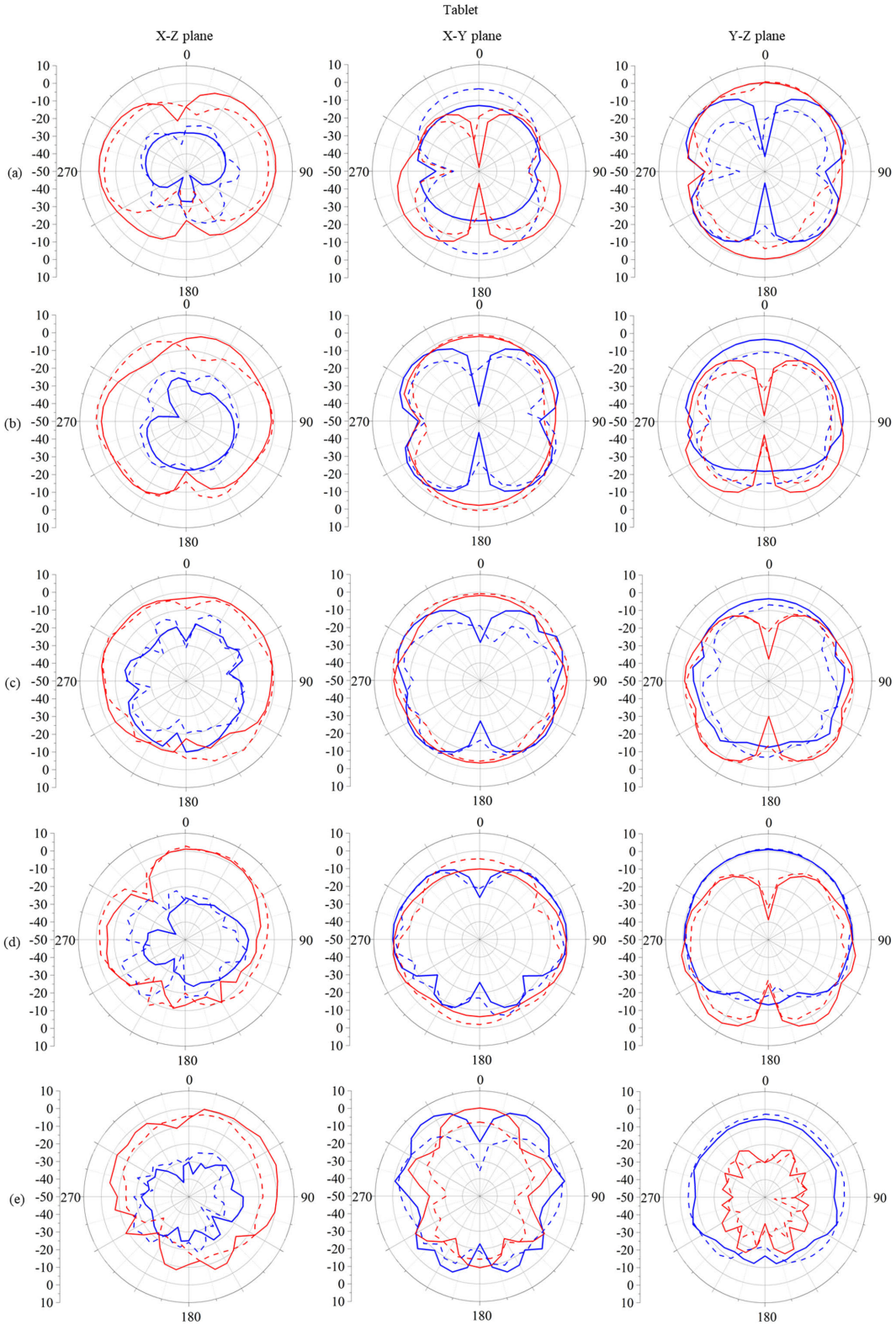

FIGURE 20. 2D Radiation pattern of a tablet MIMO antenna system: (a)900 MHz, (b)1020 MHz, (c)1760 MHz, (d)2420 MHz, (e)4430 MHz, (f)6250 MHz and (g)7400 MHz.

ECC results even when integrated within tablet computers or smartphones. This further verifies the MIMO antenna system's practical usefulness in many electronic gadgets.

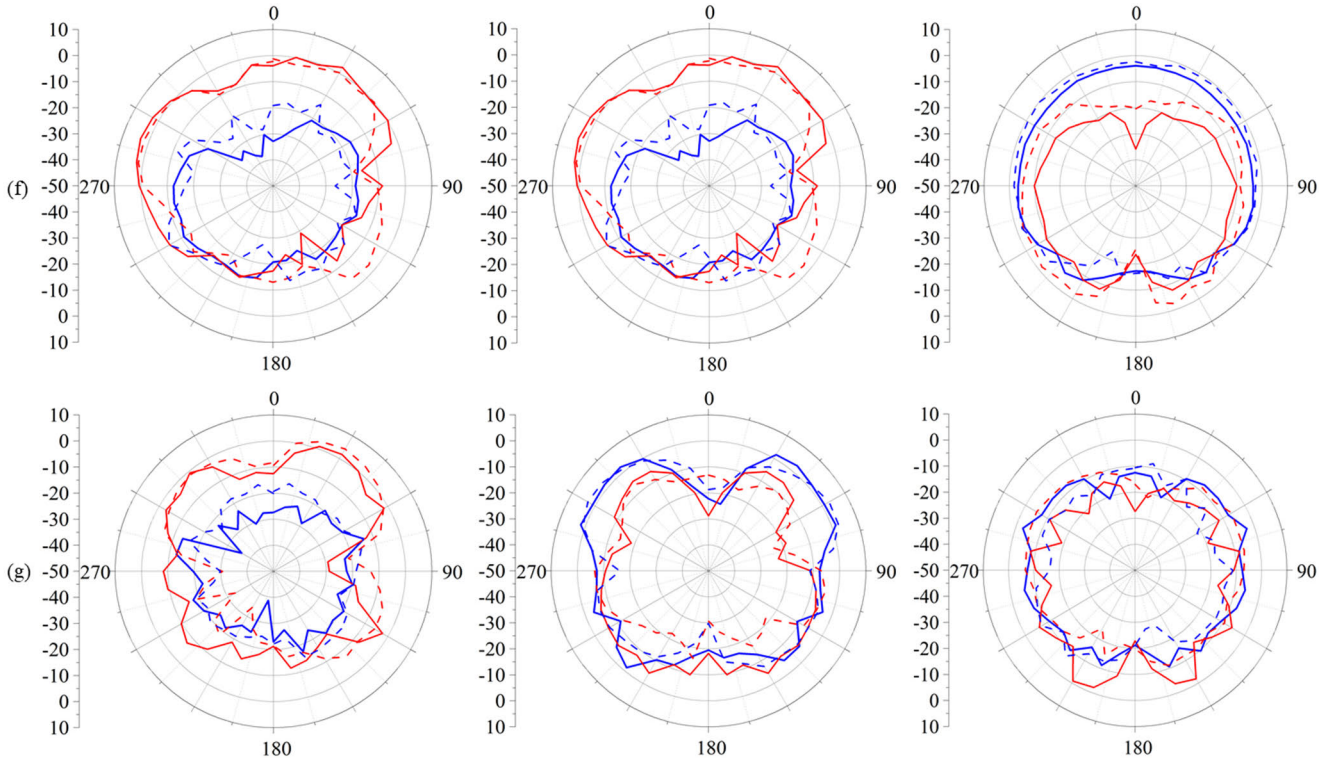

FIGURE 20. *(Continued.)* **2D Radiation pattern of a tablet MIMO antenna system: (a)900 MHz, (b)1020 MHz, (c)1760 MHz, (d)2420 MHz, (e)4430 MHz, (f)6250 MHz and (g)7400 MHz.**

Fig. 13 shows the isolation simulation and measurement results. It can be seen that the isolation in the frequency band below 1.5 GHz is relatively poor compared to other frequency bands. Therefore, the ECC of 1.5 GHz is also higher than other frequency bands. The performance of the representative MIMO antenna system is consistent with formula (2).

Based on the above analysis results of the MIMO antenna system, it is confirmed that the gain of the antenna is about 2.5dBi at low frequencies, and the efficiency is as high as about 62%, while the peak gain at high frequencies reaches about 4.1dBi, and the efficiency is as high as about 70%. In addition, the MIMO antenna system can stably keep the isolation between antennas below −10 dB, and the ECC is kept below 0.5, whether it is on a laptop, tablet, or smartphone. performance in electronic devices.

IV. HUMAN BODY EFFECT ANALYSIS

A. HUMAN BODY MODEL

Because wireless communication must be delivered via the antenna, electromagnetic radiation is produced in the process, and the MIMO antenna system is an electronic product used close to the human body, so it is important to investigate whether the MIMO antenna system has radiation hazards to the human body. In this paper, the MIMO antenna system is placed on parts of the human body that use laptops, tablets, and smartphones for simulation, such as the head, hands, and legs, as shown in Figs. 23-25, to observe the impact of the MIMO antenna system on whether the human body has health effects.

B. ANALYSIS OF THE IMPACT OF SAR ON THE HUMAN BODY

Many countries have formulated relevant regulations on the radiation value of electronic products, called Specific Absorption Rate (SAR). SAR is mainly used to assess whether electronic equipment can cause potential harm to the human body. In the United States (US), SAR is regulated by the Federal Communications Commission (FCC) guidelines, which stipulate that 1g SAR must be less than 1.6W/kg. Furthermore, according to the European Conformité Européenne (CE) rule,10g SAR must be less than 2W/kg. The above SAR value is calculated based on the power absorbed by a specific volume in a specified time, and the calculation formula is expressed in (4) [32]:

$$\mathrm{SAR} = \frac{d}{dt}\left(\frac{dw}{DM}\right) = \frac{d}{dt}\left(\frac{dW}{\rho dV}\right) \tag{4}$$

Figs. 26 and 28 show the power values of 1g SAR and 10g SAR calculated when the MIMO antenna system of a smartphone is 2mm away from the head. Here, the MIMO antenna system is hidden for easy observation. Table 2 displays the MIMO antenna system's detailed SAR values at the following frequencies. When the feeding power is 0.1W (20dBm), several important frequencies 900MHz and 1.02, 1.76, 2.42,

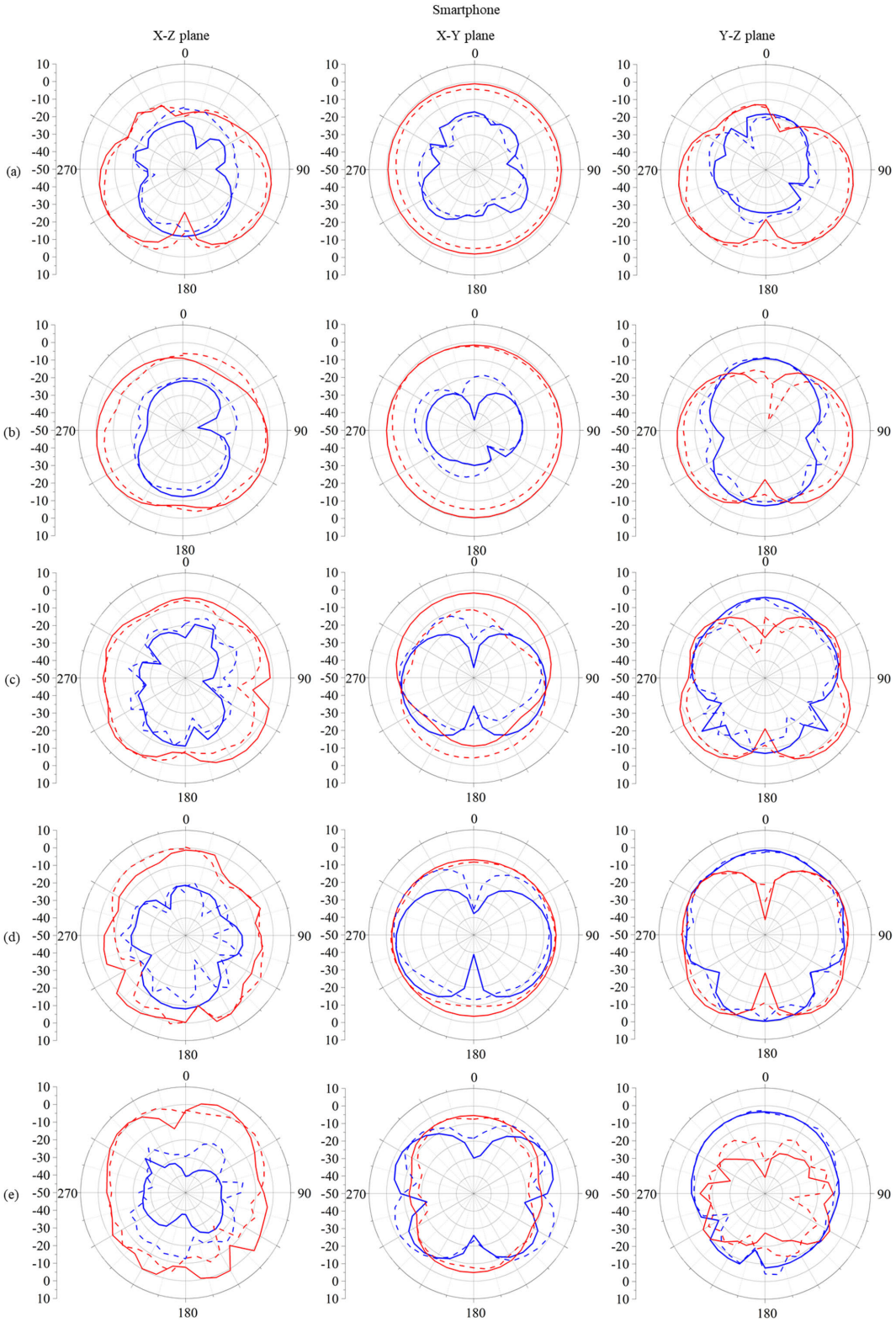

FIGURE 21. 2D Radiation Pattern of a smartphone MIMO Antenna System: (a)900 MHz, (b)1020 MHz, (c)1760 MHz, (d)2420 MHz, (e)4430 MHz, (f)6250 MHz and (g)7400 MHz.

4.43, 6.25, and 7.4 GHz of the MIMO antenna system are analyzed and simulated, respectively. Fig. 28 provides an analysis of the impact of the MIMO antenna system on the power density (PD) within human body regions of 1 cm^2 and

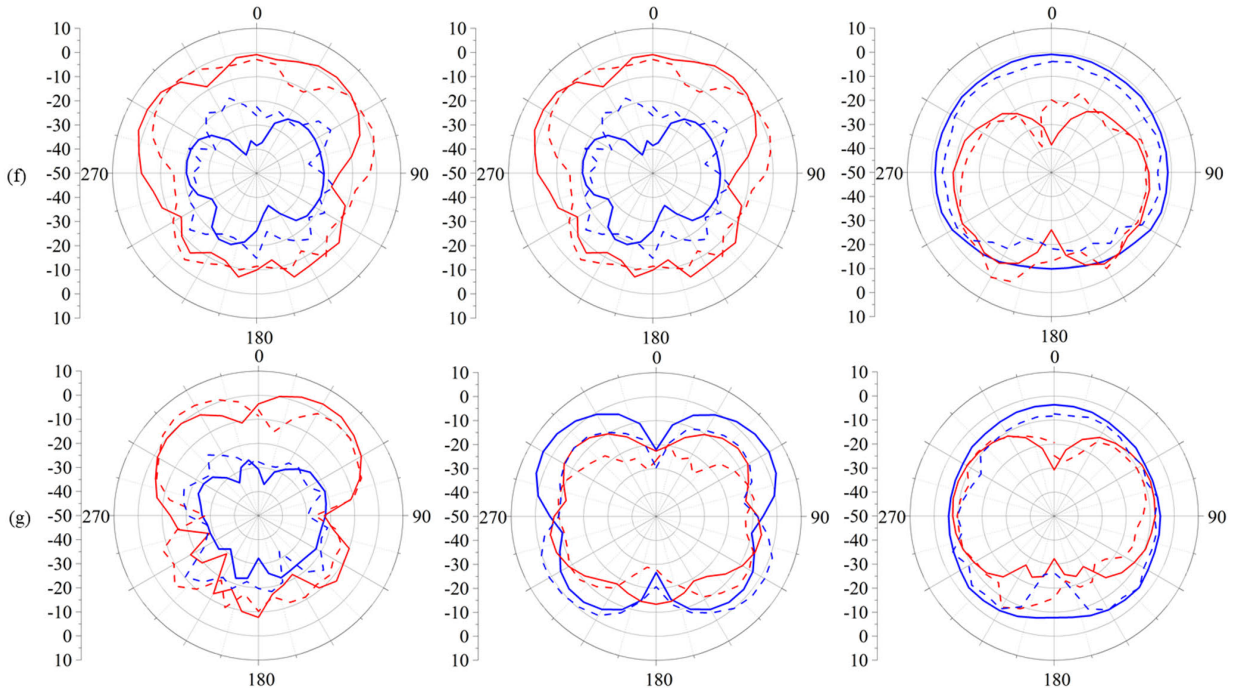

FIGURE 21. *(Continued.)* **2D Radiation Pattern of a smartphone MIMO Antenna System: (a)900 MHz, (b)1020 MHz, (c)1760 MHz, (d)2420 MHz, (e)4430 MHz, (f)6250 MHz and (g)7400 MHz.**

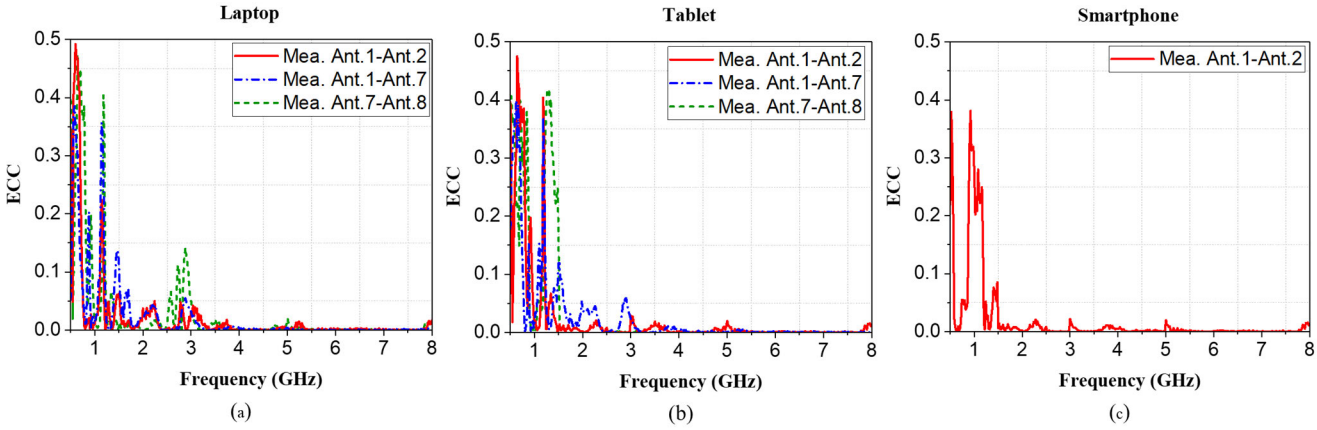

FIGURE 22. **ECC measurement results for MIMO antenna systems: (a)laptop, (b)tablet and (c)smartphone.**

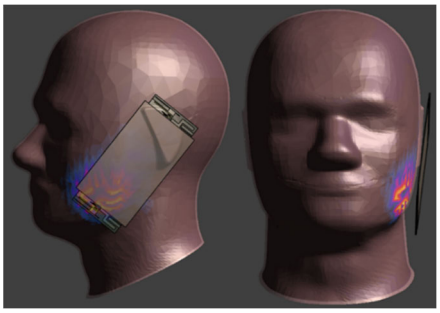

FIGURE 23. **Smartphone MIMO antenna system placed on a human head model.**

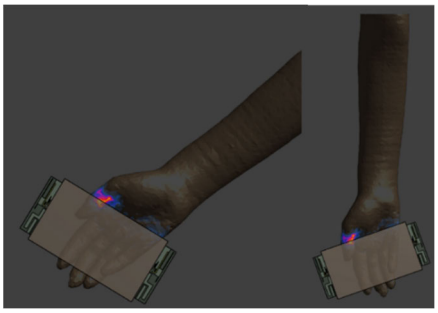

FIGURE 24. **Smartphone MIMO antenna system placed on a human hand model.**

4 cm^2 at 6.25 GHz and 7.4 GHz. Furthermore, was carried out to observe the SAR values for 1g and 10g when the power is increased from 20 dBm (0.1W) to 26 dBm (0.4W). The results in Fig. 29(a) and (b) indicate an increase in

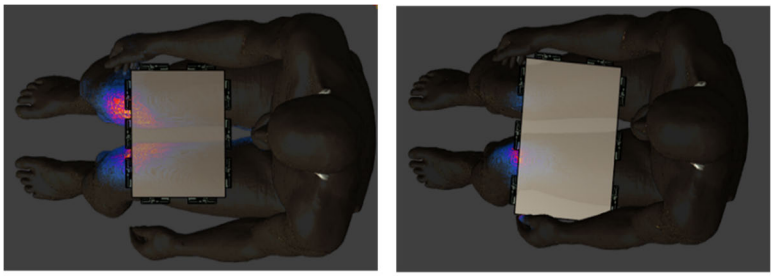

FIGURE 25. The MIMO antenna system is placed on the human leg model: (a)tablet and (b)laptop.

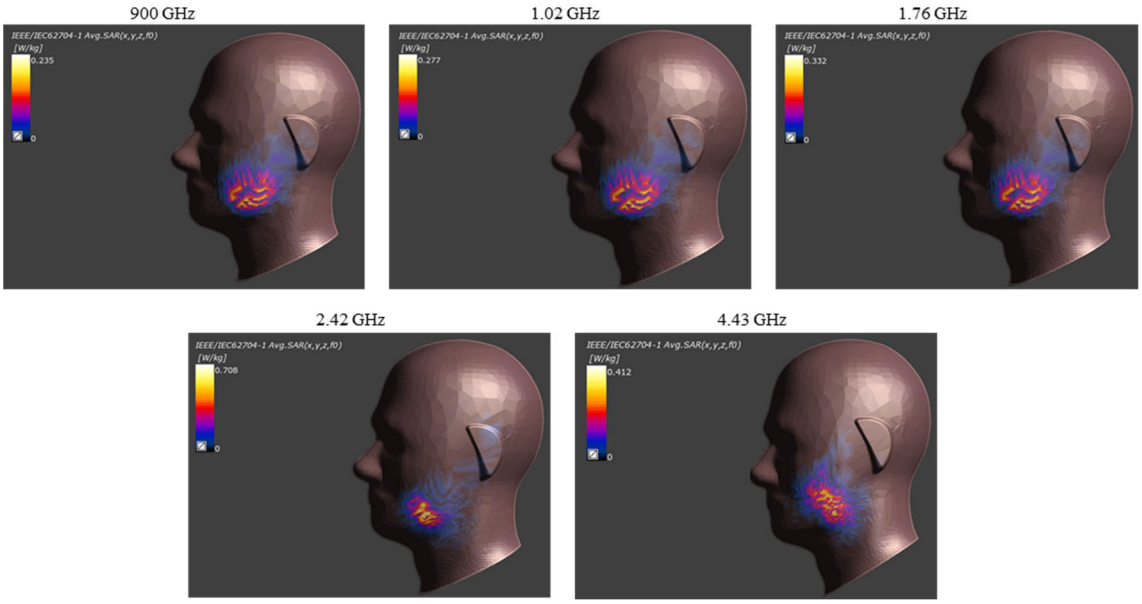

FIGURE 26. Simulated 1g SAR results of the MIMO antenna system for smartphones on the head frequencies: 900 MHz, 1.02 GHz, 1.76 GHz, 2.42 GHz and 4.43 GHz.

TABLE 2. 1G SAR and 10G SAR values of smartphone MIMO antenna system on the human head.

Frequency	1g SAR	10g SAR
900 MHz	0.235	0.134
1.02 GHz	0.277	0.168
1.76 GHz	0.332	0.202
2.42 GHz	0.708	0.476
4.43 GHz	0.412	0.294

SAR values for both 1g and 10g, but they remain within the standard range. The SAR value at 26 dBm is 0.77 higher for 1g and 0.47 higher for 10g compared to the 20 dBm SAR values. Therefore, it can be concluded that SAR values gradually increase with higher input power. After optimization adjustments, the proposed MIMO antenna system in this paper ensures that the SAR values for the MIMO antenna system deployed on various electronic devices are maintained within the standard range.

Figs. 30-38 show the SAR and PD effects of MIMO antenna systems for tablets and laptops at the positions of the hands and legs of the human body, and Table 3 to Table 5 are the detailed values of all SARs of MIMO antenna systems at the corresponding frequencies. All of the MIMO antenna system's SARs and PDs are within the specified range, and it has also been proved that the MIMO antenna system has no negative impacts on the human body.

C. COMPARISON OF PERFORMANCE WITH OTHER ANTENNAS

Table 6 compares the MIMO antenna system proposed in this paper with other literature, and Table 7 compares the frequency range covered by the MIMO antenna system

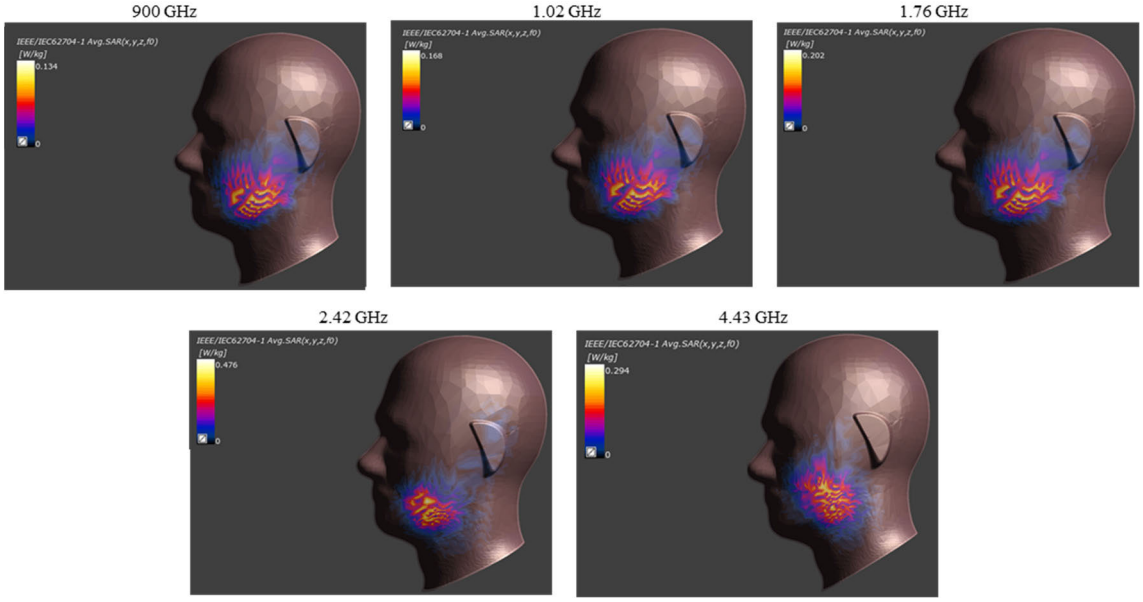

FIGURE 27. Simulated 10g SAR results of the MIMO antenna system for smartphones on the head frequencies: 900 MHz, 1.02 GHz, 1.76 GHz, 2.42 GHz and 4.43 GHz.

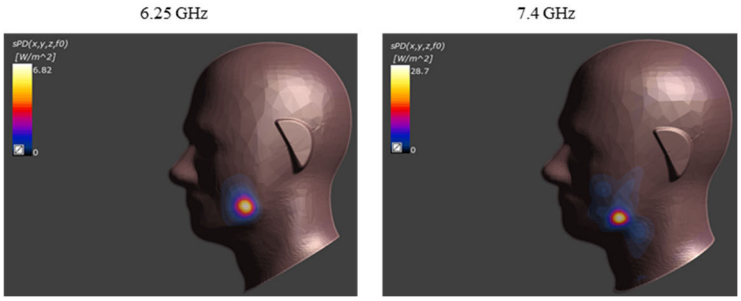

FIGURE 28. Smartphone MIMO antenna system on the head PD simulation results at 4cm2: 6.25 GHz and 7.4 GHz.

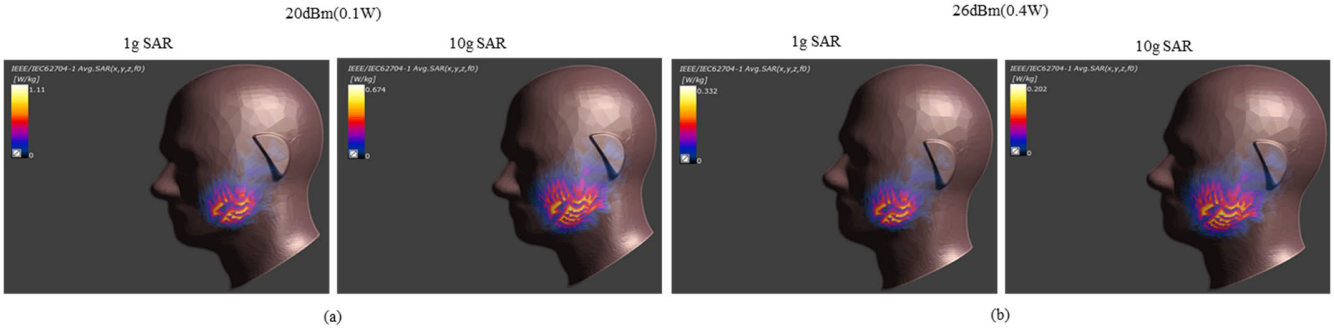

FIGURE 29. 1g SAR and 10g SAR simulation results of smartphone MIMO antenna system at head frequency 1.76 GHz: (a) 20 dBm and (b) 26 dBm.

with the antenna coverage in other literature. The comparison of Table 6 and Table 7 shows that the proposed MIMO antenna system covers many kinds of operating frequency band, including LTE900 (880-960 MHz), LTE1700 (1710-2155 MHz), LTE1800 (1710-1880 MHz), LTE1900 (1850-1990 MHz), LTE2100 (1920-2170 MHz), LTE2300 (2305-2360 MHz), LTE2500 (2496-2690 MHz), LTE2600 (2500-2690 MHz), GPS (1176 MHz, 1277 MHz), n79 (4400-5000 MHz) and WiFi 7 (6250-7150 MHz) frequency bands, and the MIMO antenna system has good isolation below −10dB. multi-band antenna MIMO also has a maximum gain of up to 4.1dBi in terms

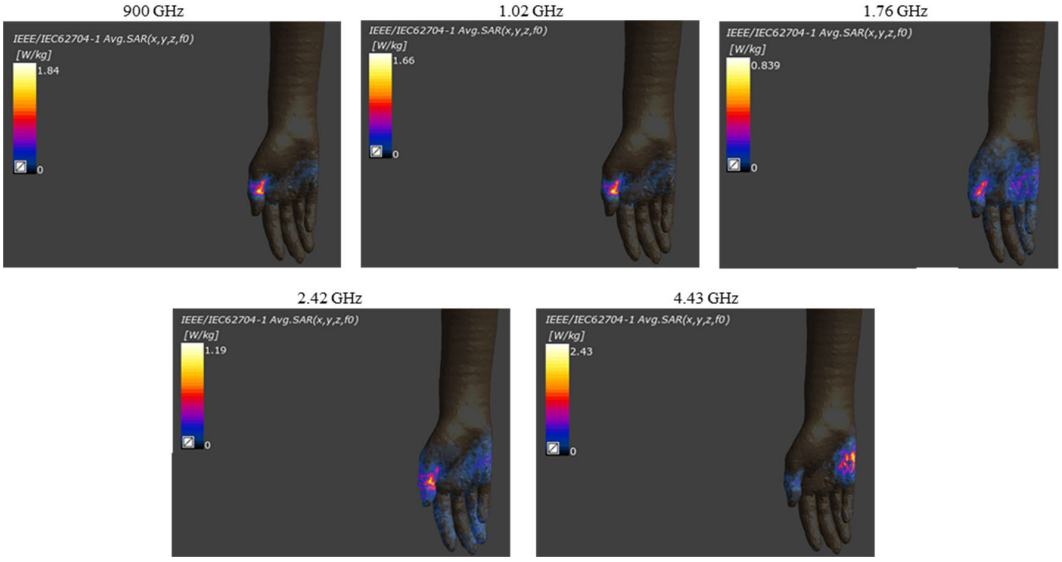

FIGURE 30. Simulated 1g SAR results of the MIMO antenna system for smartphones on the hand frequencies: 900 MHz, 1.02 GHz, 1.76 GHz, 2.42 GHz and 4.43 GHz.

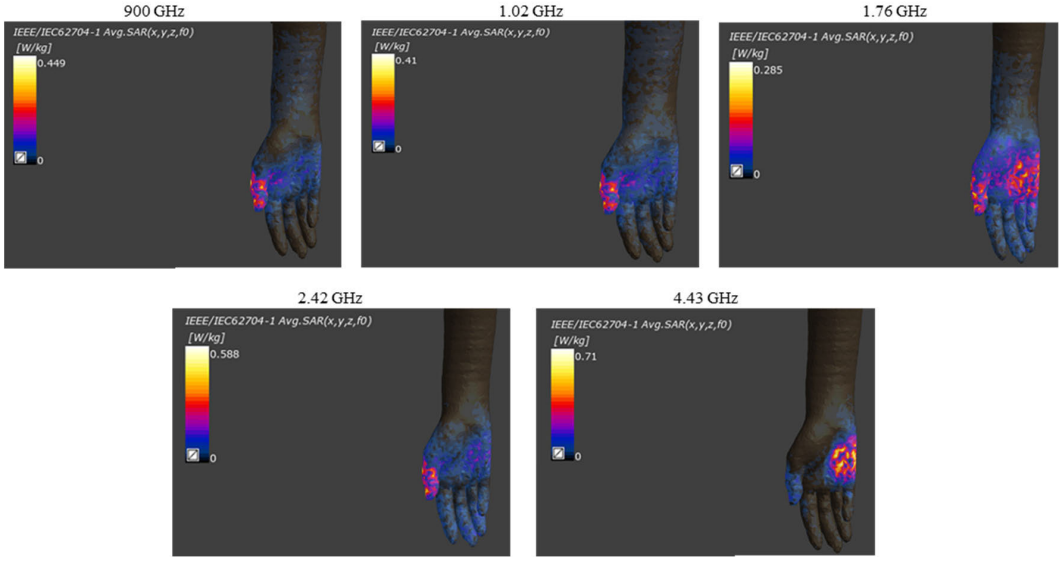

FIGURE 31. Simulated 10g SAR results of the MIMO antenna system for smartphones on the hand frequencies: 900 MHz, 1.02 GHz, 1.76 GHz, 2.42 GHz and 4.43 GHz.

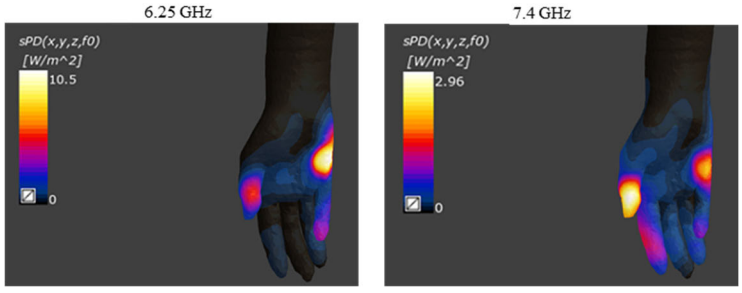

FIGURE 32. Smartphone MIMO antenna system on the hand PD simulation results at 4cm^2: 6.25 GHz and 7.4 GHz.

of performance, and the highest efficiency value is 71%, so it can be used in various electronic devices such as smartphones, tablets, and laptops. The antennas designed in [5], [8], [15], [16], [19], and [27] mainly the Sub-6G or

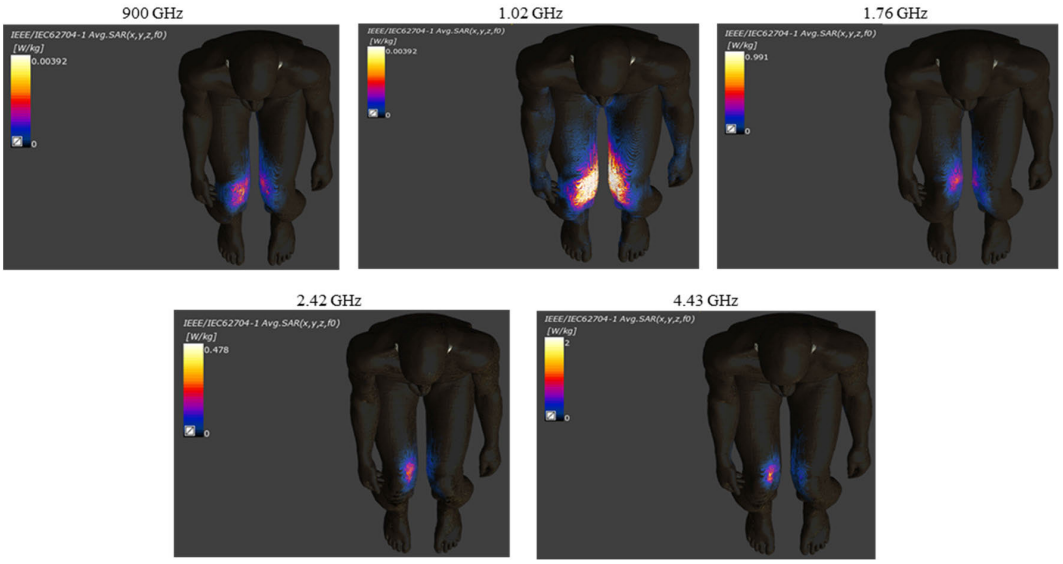

FIGURE 33. Simulated 1g SAR results of the MIMO antenna system for tablet on the leg frequencies: 900 MHz, 1.02 GHz, 1.76 GHz, 2.42 GHz and 4.43 GHz.

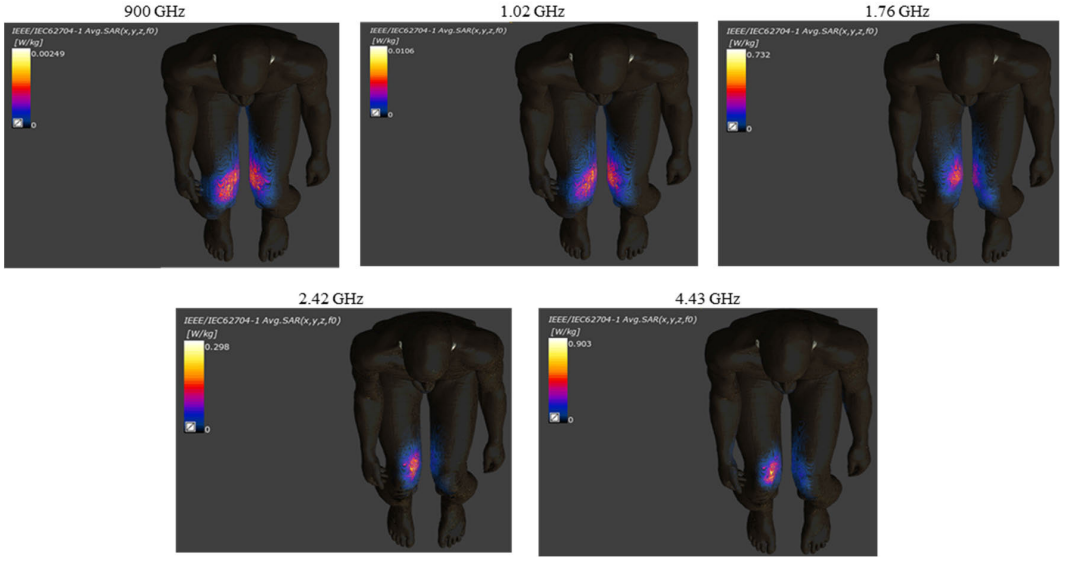

FIGURE 34. Simulated 10g SAR results of the MIMO antenna system for tablet on the leg frequencies: 900 MHz, 1.02 GHz, 1.76 GHz, 2.42 GHz and 4.43 GHz.

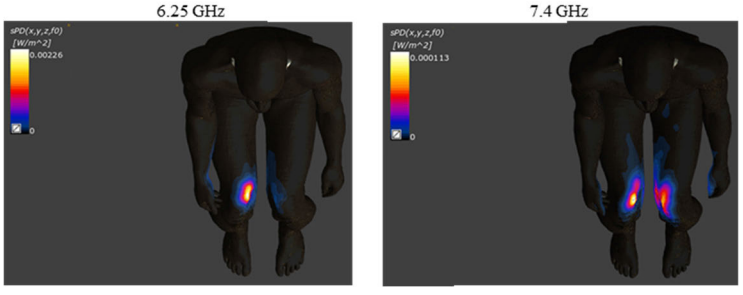

FIGURE 35. Tablet MIMO antenna system on the leg PD simulation results at 4cm^2: 6.25 GHz and 7.4 GHz.

5G frequency band and are usually only applicable to a specific single electronic device. In addition, although the antennas proposed in [9] and [17] have the working frequency band of LTE and WLAN 2.4 GHz, none of these

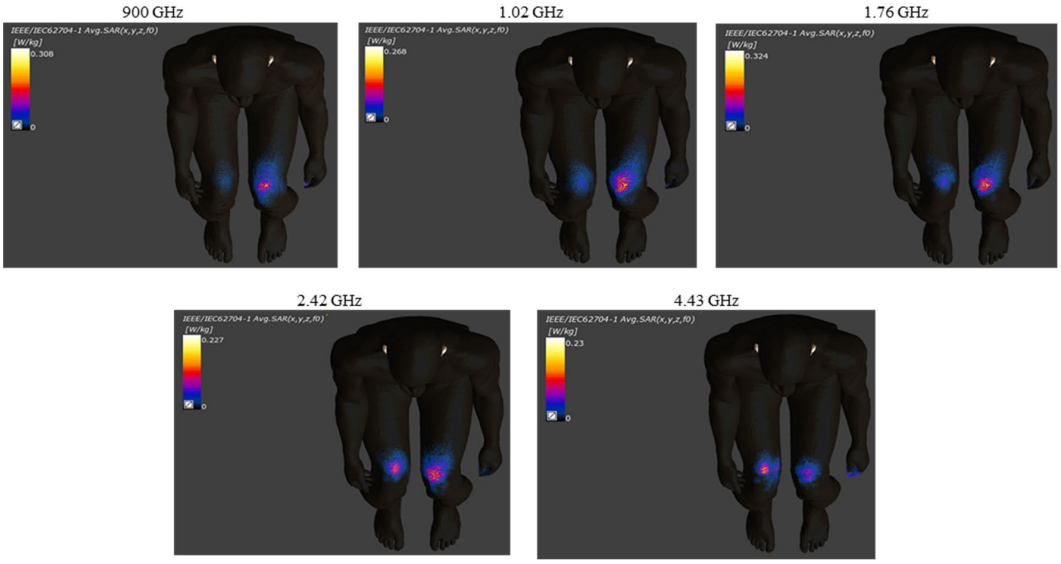

FIGURE 36. Simulated 1g SAR results of the MIMO antenna system for laptop on the leg frequencies: 900 MHz, 1.02 GHz, 1.76 GHz, 2.42 GHz and 4.43 GHz.

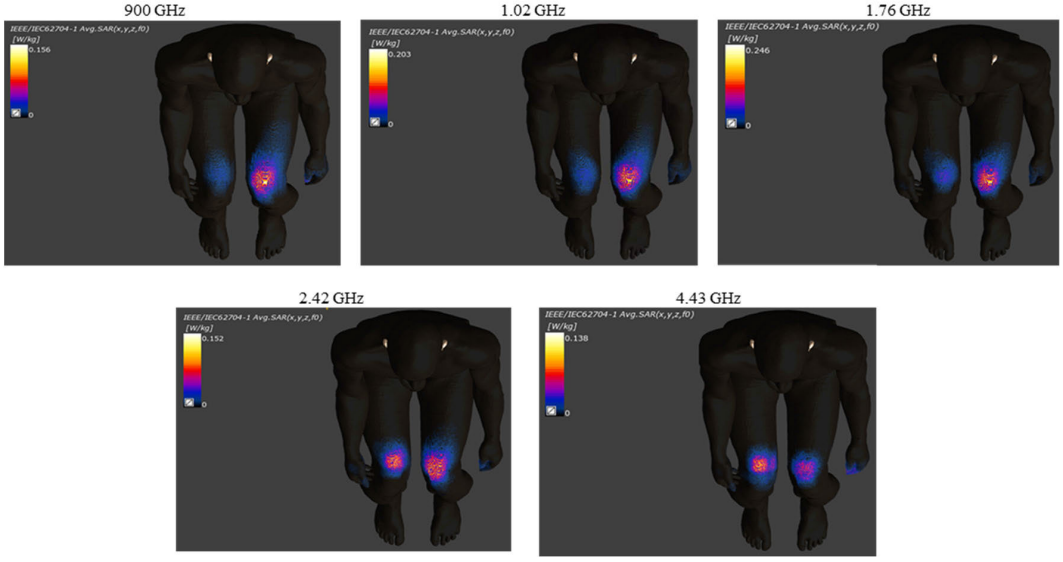

FIGURE 37. Simulated 10g SAR results of the MIMO antenna system for laptop on the leg frequencies: 900 MHz, 1.02 GHz, 1.76 GHz, 2.42 GHz and 4.43 GHz.

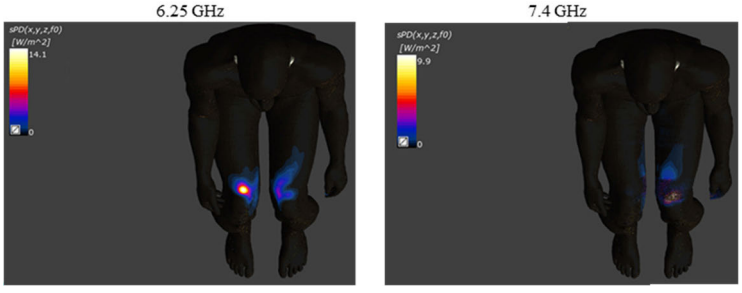

FIGURE 38. Laptop MIMO antenna system on the leg PD simulation results at 4cm^2: 6.25 GHz and 7.4 GHz.

antenna designs can cover the frequency bands of Sub-6G and WiFi 7 at the same time, and in lower frequency bands such as LTE Both require the use of passive components to achieve. On the contrary, MIMO antenna systems can

TABLE 3. 1G SAR and 10G SAR values of smartphone MIMO antenna system in the human hand.

Frequency	1g SAR	10g SAR
900 MHz	1.84	0.499
1.02 GHz	1.66	0.41
1.76 GHz	0.839	0.285
2.42 GHz	1.19	0.588
4.43 GHz	2.43	0.71

TABLE 4. 1G SAR and 10G SAR values of tablet MIMO antenna system on a human leg.

Frequency	1g SAR	10g SAR
900 MHz	0.308	0.156
1.02 GHz	0.268	0.203
1.76 GHz	0.324	0.246
2.42 GHz	0.227	0.152
4.43 GHz	0.23	0.138

TABLE 5. 1G SAR and 10G SAR values of the laptop MIMO antenna system on a human leg.

Frequency	1g SAR	10g SAR
900 MHz	0..0039	0.0025
1.02 GHz	0.0039	0.0106
1.76 GHz	0.991	0.732
2.42 GHz	0.478	0.298
4.43 GHz	2	0.903

TABLE 6. Performance comparison of the proposed MIMO antenna system with antennas in the literature.

Ref.	Size (mm)	Applied to	Operating Band (MHz)	Efficiency (%)	Isolation (dB)	Gain (dBi)	MIMO
[10]	150x75x0.8	Smartphone	3200-7300	≧61	-12	-	8x8
[4]	4x19x0.8	Smartphone	3400-3600	≧41	-12	-	8x8
			4800-5000	≧38	-15		
[5]	21.8x7x2	Smartphone	3300-3600	≧71	-24	-	8x8
			4400-5000	≧68	-26		
[13]	15x3x0.4	Laptop	3400-3800	≧42	-10	-	4x4
			4800-5000				
[14]	130x3x0.4	Laptop	700-900	40-65	-15	0.5-1.9	2x2
			1800-250	51-73		1.8-3.8	
[19]	22.3x3.5x 0.4	Laptop	2400-2485	≧78	-	4.6	-
			4740-7260				
[21]	13.9x7x0.8	Smartphone	3100-6000	41-69	-10	-	8x8
[29]	150x80x0.8	Smartphone	3400-3600	62-76	-17.5	-	8x8
Proposed antenna	12.5x60x0.8	Smartphone	880-960	≧62	-17	2.5	2x2
		Tablet	1710-2690	≧80	-18	4.4	10x10
		Laptop	4400-5000	≧64	-18	2.7	
			6250-7150	≧71	-18	4.1	

TABLE 7. Comparison of the covered frequency bands between the proposed MIMO antenna system and the antennas in the literature.

Ref.	LTE 880-960 MHz	LTE 1700-2600 MHz	WLAN 2400-2462 MHz	Sub-6G 4400-500 MHz	WiFi-6E 6250-7150 MHz
[10]	-	-	-	Supported	Supported
[4]	-	-	-	Supported	-
[5]	-	-	-	Supported	-
[13]	-	-	-	Supported	-
[14]	Supported	Supported	-	-	-
[19]	-	-	Supported	-	Supported
[21]	-	-	-	-	-
[29]	-	-	-	Supported	-
Proposed antenna	Supported	Supported	Supported	Supported	Supported

simultaneously implement multiple frequency bands from LTE to Sub-6G and WiFi 7 without any passive components to achieve the required frequency bands. The MIMO antenna system shows ideal results in terms of frequency coverage,

isolation, and antenna performance, and is versatile enough to be adapted to different electronic devices without affecting antenna performance.

V. CONCLUSION

This paper proposes a MIMO antenna system that applies to various electronic devices such as laptops, tablets, and smartphones, covers multiple frequency bands at the same time, and the antenna also complies with the SAR and PD standards and does not affect human health. Through the simple coupled-feed structure, the multi-band antenna realizes the LTE frequency band at the same time without using any passive components, and realizes the Sub-6G and WiFi 7 working frequency bands by the monopole antenna structure, while stably maintaining the isolation below −10dB degree and good antenna performance. The MIMO antenna system has shown good efficiency and gained results in measurement. To reduce costs and make the adjustment of the proposed antenna simpler, no passive components are added to the design. Because the antenna cannot cover all LTE frequency bands in a limited space. However, without considering the cost factor, there are ways to make the antenna include lower frequency bands by appropriately adding passive components and adjusting them. When the MIMO antenna system is configured on electronic devices of different sizes, it can still retain all expected frequency bands and antenna performance, showing excellence and stability. Finally, the MIMO antenna system proposed in this paper can be applied to various electronic devices with a simple structure, to adapt to ever-changing portable devices in the future and greatly improve the practical performance of mobile communication.

REFERENCES

[1] H. Aliakbari, L. Y. Nie, and B. K. Lau, "Large screen enabled tri-port MIMO handset antenna for low LTE bands," *IEEE Open J. Antennas Propag.*, vol. 2, pp. 911–920, 2021, doi: 10.1109/OJAP.2021.3107436.

[2] N. Jaglan, S. D. Gupta, and M. S. Sharawi, "18 element massive MIMO/diversity 5G smartphones antenna design for sub-6 GHz LTE bands 42/43 applications," *IEEE Open J. Antennas Propag.*, vol. 2, pp. 533–545, 2021, doi: 10.1109/OJAP.2021.3074290.

[3] X.-T. Yuan, Z. Chen, T. Gu, and T. Yuan, "A wideband PIFA-pair-based MIMO antenna for 5G smartphones," *IEEE Antennas Wireless Propag. Lett.*, vol. 20, no. 3, pp. 371–375, Mar. 2021, doi: 10.1109/LAWP.2021.3050337.

[4] C. Deng, X. Cao, D. Li, and W. Yu, "Compact dual-band MIMO antenna with shared decoupling structure for 5G mobile terminals," *IEEE Antennas Wireless Propag. Lett.*, vol. 22, no. 6, pp. 1281–1285, Jun. 2023, doi: 10.1109/LAWP.2023.3240673.

[5] W. Hu, Q. Li, H. Wu, Z. Chen, L. Wen, W. Jiang, and S. Gao, "Dual-band antenna pair with high isolation using multiple orthogonal modes for 5G smartphones," *IEEE Trans. Antennas Propag.*, vol. 71, no. 2, pp. 1949–1954, Feb. 2023, doi: 10.1109/TAP.2022.3233458.

[6] Y. Fang, Y. Liu, Y. Jia, J. Liang, and H. H. Zhang, "Reconfigurable structure reutilization low-SAR MIMO antenna for 4G/5G full-screen metal-frame smartphone operation," *IEEE Antennas Wireless Propag. Lett.*, vol. 22, no. 5, pp. 1219–1223, May 2023, doi: 10.1109/LAWP.2023.3236782.

[7] W. Jiang, B. Liu, Y. Cui, and W. Hu, "High-isolation eight-element MIMO array for 5G smartphone applications," *IEEE Access*, vol. 7, pp. 34104–34112, 2019, doi: 10.1109/ACCESS.2019.2904647.

[8] S. Padmanathan, A. Abdullah Al-Hadi, A. M. Elshirkasi, S. S. Al-Bawri, M. T. Islam, T. Sabapathy, M. Jusoh, P. Akkaraekthalin, and P. J. Soh, "Compact multiband reconfigurable MIMO antenna for sub-6GHz 5G mobile terminal," *IEEE Access*, vol. 10, pp. 60241–60252, 2022, doi: 10.1109/ACCESS.2022.3180048.

[9] A. Zhao and Z. Ren, "Wideband MIMO antenna systems based on coupled-loop antenna for 5G N77/N78/N79 applications in mobile terminals," *IEEE Access*, vol. 7, pp. 93761–93771, 2019, doi: 10.1109/ACCESS.2019.2913466.

[10] A. K. Rai, R. K. Jaiswal, K. Kumari, K. V. Srivastava, and C.-Y.-D. Sim, "Wideband monopole eight-element MIMO antenna for 5G mobile terminal," *IEEE Access*, vol. 11, pp. 689–696, 2023, doi: 10.1109/ACCESS.2022.3232698.

[11] B. Yang, Y. Xu, J. Tong, Y. Zhang, Y. Feng, and Y. Hu, "Tri-port antenna with shared radiator and self-decoupling characteristic for 5G smartphone application," *IEEE Trans. Antennas Propag.*, vol. 70, no. 6, pp. 4836–4841, Jun. 2022, doi: 10.1109/TAP.2021.3137378.

[12] H. V. Singh, D. V. S. Prasad, and S. Tripathi, "Compact tightly-coupled self-decoupled MIMO antenna using internal hybrid tunning," *IEEE Trans. Circuits Syst. II, Exp. Briefs*, vol. 69, no. 12, pp. 4794–4798, Dec. 2022, doi: 10.1109/TCSII.2022.3196791.

[13] S.-C. Chen, J.-L. Zhu, and Chung-I. G. Hsu, "Compact double shorted loop sub-6-GHz dual-band MIMO quad-antenna system," *IEEE Access*, vol. 9, pp. 114672–114679, 2021, doi: 10.1109/ACCESS.2021.3104306.

[14] S.-C. Chen and M.-C. Hsu, "LTE MIMO closed slot antenna system for laptops with a metal cover," *IEEE Access*, vol. 7, pp. 28973–28981, 2019, doi: 10.1109/ACCESS.2019.2901964.

[15] J. Choi, W. Hwang, C. You, B. Jung, and W. Hong, "Four-element reconfigurable coupled loop MIMO antenna featuring LTE full-band operation for metallic-rimmed smartphone," *IEEE Trans. Antennas Propag.*, vol. 67, no. 1, pp. 99–107, Jan. 2019, doi: 10.1109/TAP.2018.2877299.

[16] H. Aliakbari and B. K. Lau, "Low-profile two-port MIMO terminal antenna for low LTE bands with wideband multimodal excitation," *IEEE Open J. Antennas Propag.*, vol. 1, pp. 368–378, 2020, doi: 10.1109/OJAP.2020.3010916.

[17] J. Kulkarni, N. Kulkarni, and A. Desai, "Development of 'H-shaped' monopole antenna for IEEE 802.11 a and HIPERLAN 2 applications in the laptop computer," *Int. J. RF Microw. Comput.-Aided Eng.*, vol. 30, no. 7, Jul. 2020, Art. no. e22233, doi: 10.1002/mmce.22233.

[18] J. Kulkarni, A. G. Alharbi, A. Desai, C.-Y.-D. Sim, and A. Poddar, "Design and analysis of wideband flexible self-isolating MIMO antennas for sub-6 GHz 5G and WLAN smartphone terminals," *Electronics*, vol. 10, no. 23, p. 3031, Dec. 2021, doi: 10.3390/electronics10233031.

[19] C.-Y.-D. Sim, J. Kulkarni, S.-H. Wang, S.-Y. Zheng, Z.-H. Lin, and S.-C. Chen, "Low-profile laptop antenna design for Wi-Fi 6E band," *IEEE Antennas Wireless Propag. Lett.*, vol. 22, no. 1, pp. 79–83, Jan. 2023, doi: 10.1109/LAWP.2022.3202697.

[20] S.-W. Su, C.-T. Lee, and S.-C. Chen, "Compact, printed, tri-band loop antenna with capacitively-driven feed and end-loaded inductor for notebook computer applications," *IEEE Access*, vol. 6, pp. 6692–6699, 2018, doi: 10.1109/ACCESS.2018.2794606.

[21] C.-Y.-D. Sim, H.-Y. Liu, and C.-J. Huang, "Wideband MIMO antenna array design for future mobile devices operating in the 5G NR frequency bands n77/n78/n79 and LTE band 46," *IEEE Antennas Wireless Propag. Lett.*, vol. 19, no. 1, pp. 74–78, Jan. 2020, doi: 10.1109/LAWP.2019.2953334.

[22] Y. Liu, W. Cui, Y. Jia, and A. Ren, "Hepta-band metal-frame antenna for LTE/WWAN full-screen smartphone," *IEEE Antennas Wireless Propag. Lett.*, vol. 19, no. 7, pp. 1241–1245, Jul. 2020, doi: 10.1109/LAWP.2020.2996712.

[23] Z.-Q. Xu, Q.-Q. Zhou, Y.-L. Ban, and S. S. Ang, "Hepta-band coupled-fed loop antenna for LTE/WWAN unbroken metal-rimmed smartphone applications," *IEEE Antennas Wireless Propag. Lett.*, vol. 17, no. 2, pp. 311–314, Feb. 2018, doi: 10.1109/LAWP.2017.2787863.

[24] D. Huang and Z. Du, "Eight-band antenna with a small ground clearance for LTE metal-frame mobile phone applications," *IEEE Antennas Wireless Propag. Lett.*, vol. 17, no. 1, pp. 34–37, Jan. 2018, doi: 10.1109/LAWP.2017.2772303.

[25] P. Lin and K. Wong, "Low-profile multibranch monopole antenna with integrated matching circuit for LTE/WWAN/WLAN operation in the tablet computer," *Microw. Opt. Technol. Lett.*, vol. 56, no. 7, pp. 1662–1666, Jul. 2014, doi: 10.1002/mop.28404.

[26] R. Ullah, S. Ullah, R. Ullah, F. Faisal, I. B. Mabrouk, and M. J. A. Hasan, "A 10-ports MIMO antenna system for 5G smartphone applications," *IEEE Access*, vol. 8, pp. 218477–218488, 2020, doi: 10.1109/ACCESS.2020.3042750.
[27] J. Dong, S. Wang, and J. Mo, "Design of a twelve-port MIMO antenna system for multi-mode 4G/5G smartphone applications based on characteristic mode analysis," *IEEE Access*, vol. 8, pp. 90751–90759, 2020, doi: 10.1109/ACCESS.2020.2994068.
[28] Z. Ji, Y. Guo, Y. He, L. Zhao, G.-L. Huang, C. Zhou, Q. Zhang, and W. Lin, "Low mutual coupling design for 5G MIMO antennas using multi-feed technology and its application on metal-rimmed mobile phones," *IEEE Access*, vol. 9, pp. 151023–151036, 2021, doi: 10.1109/ACCESS.2021.3126640.
[29] Y. Li, C.-Y.-D. Sim, Y. Luo, and G. Yang, "High-isolation 3.5 GHz eight-antenna MIMO array using balanced open-slot antenna element for 5G smartphones," *IEEE Trans. Antennas Propag.*, vol. 67, no. 6, pp. 3820–3830, Jun. 2019, doi: 10.1109/TAP.2019.2902751.
[30] Z. Feng, G. You-Gang, A. L. Rao, S. Dan, S. Yuan-Mao, Z. Ying-Yan, and M. Ai-Li, "Distance boundary of antenna isolation calculation in engineering," in *Proc. 31st URSI Gen. Assem. Sci. Symp.*, 2014, pp. 1–4, doi: 10.1109/ursigass.2014.6929535.
[31] H. Wang, R. Zhang, Y. Luo, and G. Yang, "Compact eight-element antenna array for triple-band MIMO operation in 5G mobile terminals," *IEEE Access*, vol. 8, pp. 19433–19449, 2020, doi: 10.1109/ACCESS.2020.2967651.
[32] M.-A. Chung and C.-W. Hsiao, "Dual-band 6 × 6 MIMO antenna system for glasses applications compatible with Wi-Fi 6E and 7 wireless communication standards," *Electronics*, vol. 11, no. 5, p. 806, Mar. 2022, doi: 10.3390/electronics11050806.

MING-AN CHUNG (Member, IEEE) received the B.Eng. and M.Eng. degrees in electronic engineering from Chang Gung University, Taoyuan, Taiwan, in 2003 and 2005, respectively, and the D.Eng. degree in electrical engineering from the National Taiwan University of Science and Technology, Taipei City, Taiwan, in 2016. He is currently an Associate Professor with the Department of Electronic Engineering, National Taipei University of Technology, Taipei City, where he is also the Leader of the Innovation Wireless Communication and Electromagnetic Applications Laboratory. His research interests include wireless communication propagation, intelligent robotics, self-driving vehicles, antenna design for various mobile and wireless communications, and electromagnetic theory and applications. He is a Reviewer of many scientific journals, including IEEE TRANSACTIONS ON ANTENNAS AND PROPAGATION, IEEE TRANSACTIONS ON INDUSTRIAL INFORMATICS, *Journal of Intelligent and Robotic Systems*, *IET Microwaves, Antennas and Propagation*, IEEE ANTENNAS AND WIRELESS PROPAGATION LETTERS, *International Review of Electrical Engineering*, *International Journal on Communications Antenna and Propagation*, and *AEÜ-International Journal of Electronics and Communications*, and many international conferences, including ICRA, ICCE-TW, RFIT, ICBEB, EMCAR, and SNSP.

CHIA-CHUN HSU received the Associate degree in computer and communication engineering from Army Academy R.O.C., Taiwan, in 2015. Her current research interests include antennas, MIMO antenna system design, AIoT, and emotion recognition applications.

MING-CHANG LEE received the B.S. degree from the Taipei University of Marine Technology, in 2009, and the M.S. degree from the National Taipei University of Technology, in 2023. His research interests include composite material antenna design, switched-beam antenna systems, MIMO antenna systems, millimeter wave antenna design, and phased array antenna.

CHIA-WEI LIN received the B.S. and M.S. degrees from Chung Yuan Christian University, in 2007. He is currently pursuing the Ph.D. degree in electrical engineering with the National Taipei University of Technology. His research interests include wireless communication propagation research, antenna design, intelligent robotics research, self-driving vehicle research, embedded systems, and deep learning.